Rice

RESEARCH Open Access

OsSNDP4, a Sec14-nodulin Domain Protein, is Required for Pollen Development in Rice

Weitao Xu[1†], Xiaoqun Peng[1†], Yiqi Li[1†], Xinhuang Zeng[1], Wei Yan[1,3], Changjian Wang[1], Cheng Rui Wang[1], Shunquan Chen[3], Chunjue Xu[3*] and Xiaoyan Tang[1,2,3*]

Abstract

Pollen is encased in a robust wall that shields the male gametophyte from various stresses and aids in pollination. The pollen wall consists of gametophyte-derived intine and sporophyte-derived exine. The exine is mainly composed of sporopollenin, which is biopolymers of aliphatic lipids and phenolics. The process of exine formation has been the subject of extensive research, yet the underlying molecular mechanisms remain elusive. In this study, we identified a rice mutant of the *OsSNDP4* gene that is impaired in pollen development. We demonstrated that OsSNDP4, a putative Sec14-nodulin domain protein, exhibits a preference for binding to phosphatidylinositol (3)-phosphate [PI(3)P], a lipid primarily found in endosomal and vacuolar membranes. The OsSNDP4 protein was detected in association with the endoplasmic reticulum (ER), vacuolar membranes, and the nucleus. *OsSNDP4* expression was detected in all tested organs but was notably higher in anthers during exine development. Loss of *OsSNDP4* function led to abnormal vacuole dynamics, inhibition in Ubisch body development, and premature degradation of cellular contents and organelles in the tapetal cells. Microspores from the *ossndp4* mutant plant displayed abnormal exine formation, abnormal vacuole enlargement, and ultimately, pollen abortion. RNA-seq assay revealed that genes involved in the biosynthesis of fatty acid and secondary metabolites, the biosynthesis of lipid polymers, and exosome formation were enriched among the down-regulated genes in the mutant anthers, which correlated with the morphological defects observed in the mutant anthers. Base on these findings, we propose that *OsSNDP4* regulates pollen development by binding to PI(3)P and influencing the dynamics of membrane systems. The involvement of membrane systems in the regulation of sporopollenin biosynthesis, Ubisch body formation, and exine formation provides a novel mechanism regulating pollen wall development.

Keywords Rice, OsSNDP4, Pollen exine, Sec14-nodulin domain protein, Phosphoinositide

†Weitao Xu, Xiaoqun Peng, and Yiqi Li contributed equally to this work.

*Correspondence:
Chunjue Xu
xch@frontier-ag.com
Xiaoyan Tang
txy@frontier-ag.com
[1]Guangdong Provincial Key Laboratory of Biotechnology for Plant Development, School of Life Sciences, South China Normal University, Guangzhou, China
[2]Guangdong Laboratory for Lingnan Modern Agriculture, Guangzhou, China
[3]Shenzhen Institute of Molecular Crop Design, Shenzhen, China

Background

Pollen development is fundamental to the reproductive success of flowering plants. Pollen is developed inside the anther, the male reproductive organ of flowering plants. The anther has four layers of wall cells, from exterior to interior the epidermis, endothecium, middle layer, and tapetum, which encase a group of microspore mother cells (MMCs) prior to meiosis (Ariizumi and Toriyama 2011). These MMCs undergo meiosis, resulting in four haploid microspores. Each microspore matures into a pollen grain that contains a large vegetative cell and two small sperm cells. The tapetum plays a pivotal role in supplying nutrients for pollen development and gradually degenerates as the pollen matures (Zhang et al. 2011).

A mature pollen grain is encased in a robust wall, which is divided into the outer exine and the inner intine (Ariizumi and Toriyama 2011). The exine consists of an outer layer named the tectum, an inner layer named the nexine, and radially oriented bacula that bridge the tectum and nexine (Ariizumi and Toriyama 2011; Shi et al. 2015). The exine is primarily composed of chemically and physically stable biopolymers of aliphatic lipids and phenolics that are known as sporopollenin (Grienenberger and Quilichini 2021). The spaces between the tectum and bacula are usually filled with the tryphine, also referred to as the pollen coat (Qiao et al. 2023). Underneath the nexine lies the intine, which is immediately adjacent to the plasma membrane of the pollen vegetative cell (Ariizumi and Toriyama 2011; Shi et al. 2015). The intine is formed by the microspore after the first mitotic division. The primary constituents of the intine are pectin, cellulose, hemicellulose, hydrolytic enzymes, and hydrophobic proteins, resembling the composition of the primary cell wall of regular vegetative cells (Ariizumi and Toriyama 2011). The pollen wall is crucial to pollen function by protecting the male gametophytes from environmental stresses and facilitating pollination and pollen-stigma interaction (Shi et al. 2015).

The tapetal cells play a pivotal role in pollen wall development by synthesizing and transporting sporopollenin precursors and pollen coat compounds to the pollen surface (Ariizumi and Toriyama 2011; Shi et al. 2015). Genetic studies of male sterility genes have identified a list of evolutionally conserved genes that are presumed to play roles in the biosynthesis of aliphatic lipids and phenolic compounds that are required for pollen exine development (Wan et al. 2020). For instance, aldehyde decarbonylases such as AtCER1, OsCER1 and OsWDA1 (Aarts et al. 1997; Jung et al. 2006; Ni et al. 2018), the fatty acid hydroxylase AtCER3 (Rowland et al. 2007), the 3-Keto-acyl-CoA synthase CER6/CUT1 (Fiebig et al. 2000), and the long-chain acyl-CoA synthetases AtLACS1 and AtLACS4 (Jessen et al. 2011), are probably involved in the biosynthesis of very-long-chain fatty acids and alkanes. *OsNP1* in rice and its ortholog in maize *ZmIPE1* encode putative glucose-methanol-choline (GMC) oxidoreductases that probably have a role in hydroxylation of long-chain fatty acid at the ω-position (Chang et al. 2016a; Chen et al. 2017). The product of GMC oxidoreductase may serve as a substrate for cytochrome P450 proteins such as the Arabidopsis CYP704B1 and CYP703A2 and their rice orthologs OsCYP704B2 and OsCYP703A3 that can catalyze in-chain hydroxylation or the formation of ω-dicarboxylic fatty acids (Morant et al. 2007; Dobritsa et al. 2009; Li et al. 2010a; Yang et al. 2014). Arabidopsis AtGPAT1, AtGPAT6 and rice OsGPAT3 are all putative glycerol-3-phosphate acyltransferases that are believed to be involved in the biosynthesis of glycerolipid, a component of sporopollenin (Zheng et al. 2003; Li et al. 2012, 2019; Men et al. 2017; Sun et al. 2018). Rice *DPW2* encodes a hydroxycinnamoyl-CoA:ω-hydroxy fatty acid transferase that may contribute to the biosynthesis of phenolics (Xu et al. 2017). Arabidopsis *ACOS5* and its rice ortholog *OsACOS12* encode acyl-CoA synthetases that can convert medium- and long-chain fatty acids into fatty acyl-CoA esters (de Azevedo et al. 2009; Li et al. 2016; Yang et al. 2017), which can then be condensed to malonyl-CoA by polyketide synthases encoded by Arabidopsis *PKSA/LAP6* and *PKSB/LAP5* and their rice orthologs *OsPKS1* and *OsPKS2* (Dobritsa et al. 2010; Kim et al. 2010; Zhu et al. 2017), and subsequently reduced by tetraketide reductases encoded by Arabidopsis *TKPR1* and *TKPR2* and rice *OsTKPR1* (Grienenberger et al. 2010; Xu et al. 2019). These genes are presumed to be involved in the biosynthesis of sporopollenin precursors and/or the pollen coat compounds (Wan et al. 2020; Qiao et al. 2023).

Molecular genetic studies of male sterility genes have also identified a number of genes that are presumed to play a role in the transport of materials essential for pollen exine development. These include ABC transporters such as AtABCG11 (Panikashvili et al. 2010), AtABCG26 (Quilichini et al. 2010, 2014), AtABCG9, AtABCG31 (Choi et al. 2014), AtABCG1 and AtABCG16 (Yadav et al. 2014) in Arabidopsis, as well as OsABCG15 (Qin et al. 2013; Niu et al. 2013a; Wu et al. 2014), OsABCG26 (Zhao et al. 2015; Chang et al. 2016b), and OsABCG3 (Chang et al. 2018) in rice. In addition, a number of nonspecific lipid transfer proteins (LTPs) that are widely conserved across different plant species have also been found to be important for pollen exine development (Fang et al. 2023). These include proteins such as OsC6 (Zhang et al. 2010) and OsLTP47 (Chen et al. 2022) in rice and their Arabidopsis orthologs AtLTPg3 and AtLTPg4 (Edstam and Edqvist 2014), OsC4 and its Arabidopsis orthologs AtLTPc3 and AtLTPc1 (Huang et al. 2013), and OsEPAD1 (Li et al. 2020) and its maize orthologs ZmLTPx2 and ZmLTPg11 and wheat ortholog TaMs1 (Li et al. 2021).

In Brassica species, tapetal cells accumulate lipids and flavonoids in sub-organelles such as endoplasmic reticulum (ER)-derived tapetosomes and plastid-derived elaioplasts (Hsieh and Huang 2005; Liu and Fan 2013). These sub-organelles are released into the anther locule upon degradation of the tapetal cells, and their contents are deposited onto the pollen surface as the pollen coat (Hsieh and Huang 2007; Qiao et al. 2023). In rice, a large number of vesicles were also observed in the tapetal cells, but disruption of the tapetal cell was not observed (Zhang et al. 2011). Instead, rice plants develop Ubisch bodies, which are specialized orbicule structures on the outer surface of the tapetum (Shi et al. 2015). Ubisch bodies are thought to originate from the ER of the tapetal cells and are important for the secretion of sporopollenin precursors to the anther locule and the microspore surface (Huysmans et al. 1998). Nonetheless, the degradation of tapetal cells remains essential for pollen wall formation in rice, as indicated by the occurrence of programmed cell death signals in the tapetal cells following meiosis (Li et al. 2006, 2011; Niu et al. 2013b). Many mutants with abnormal programmed cell death also show abnormal pollen development and male sterility (Shi et al. 2015).

Plant cellular membranes are a lipid bilayer primarily composed of glycerophospholipids such as phosphatidylcholine (PC), phosphatidylserine (PS), phosphatidylethanolamine (PE), and phosphatidylinositol (PI), which provide a structural matrix for embedded proteins (Reszczyńska and Hanaka 2020). In addition to these major lipid components, plant membranes also harbor a set of minor lipids known as phosphoinositides (PIPs) that are derived from the phosphorylation of the myo-inositol head group of PI at positions D-3, 4, and 5, including PI(3)P, PI(4)P, PI(5)P, PI(3,4)P_2, PI(3,5)P_2, PI(4,5)P_2 and PI(3,4,5)P_3 (Irvine 2016; Gerth et al. 2017). PIPs are exclusively found on the cytosolic face of biological membranes and constitute less than 1% of the membrane lipid content (Gerth et al. 2017; Noack and Jaillais 2020). PIPs exhibit a strong specificity with respect to their distribution in different membrane compartments, thus providing cues to membrane identity. For instance, PI(3)P is predominantly detected in endosome and tonoplast membranes (Vermeer et al. 2006; Simon et al. 2014); PI(4)P is enriched in the membranes of the Golgi apparatus, *trans*-Golgi network, late endosome, and plasma membrane (Vermeer et al. 2009; Simon et al. 2014); and PI(4,5)P_2 is commonly found in the plasma membrane (van Leeuwen et al. 2007; Lebecq et al. 2022). These lipids play pivotal regulatory roles in controlling growth, development, and in responding to environmental cues by interacting with a multitude of proteins (Heilmann 2016; Roman-Fernandez et al. 2018).

Sec14-like PI transfer proteins (Sec14L-PITPs) comprise a group of evolutionarily conserved proteins characterized by a distinctive Sec14 domain initially identified in the yeast protein Sec14 (Holič et al. 2021). These proteins are capable of recognizing, binding, exchanging, and transferring PI, PIPs, and various other small lipophilic molecules between membranes through non-vesicular transport mechanisms (Holič et al. 2021). They are also involved in regulation of vesicular trafficking within the cell (Bankaitis et al. 2010). Sec14L-PITPs are found across all eukaryotic cells, including yeast, plants, and animals, and in each eukaryote, they form a multigene family (Montag et al. 2020). Based on their structural features, plant Sec14L-PITPs are categorized into three classes: one class contains only Sec14 domain; another class contains Sec14 domain and a plant-specific nodulin domain; and the third class contains Sec14 and Golgi dynamic (GOLD) domains (Montag et al. 2023). In vitro experiments have demonstrated PI or PC binding and transfer activities for the Sec14 domains of several Sec14L-PITPs with or without the additional domains (Huang et al. 2016b). To date, a number of plant Sec14L-PITPs have been implicated in various functions, such as chloroplast development (Hertle et al. 2020; Kim et al. 2022; Yao et al. 2023; Yang et al. 2023), polar growth of root hair cells (Grierson et al. 1997; Bohme et al. 2004; Vincent et al. 2005; Huang et al. 2013b; Ghosh et al. 2015), polar growth of pollen tubes (Moon et al. 2022), cell division and growth (Peterman et al. 2004; Tejos et al. 2017), and responses to environmental stimuli (Chu et al. 2018; Zhou et al. 2018), but none has been identified as a sporophytic factor regulating male fertility in the plant (Montag et al. 2023).

During the screening of rice mutants affecting male fertility, we identified a mutant named *ms16600* that exhibited a significant decrease in male fertility. Cloning of the mutant gene indicated that the causal mutation is in OsSNDP4, a Sec14L-PITP with both a Sec14 domain and a nodulin domain. The reduction of male fertility of *ossndp4* mutant was influenced by environment. Electron microscopy studies revealed abnormal vacuolar dynamics, irregular degradation of cellular contents, and a marked inhibition of Ubisch body formation in the tapetal cells. Additionally, the mutant plants displayed abnormal vacuole enlargement and a thinner exine in the pollen grains. A protein-lipid overlay assay indicated that OsSNDP4 has a preference for binding to PI(3)P. To date, Sec14L-PITPs and their potential binding substrates have not been implicated in the regulation of pollen exine development in any plant species, making these findings a novel contribution to our understanding of the mechanism governing pollen development.

Results

Isolation and Morphological Characterization of *ms16600* Mutant

By screening an ethyl methanesulfonate (EMS)-induced mutant library derived from the *indica* variety Huanghuazhan (HHZ) (Chen et al. 2014), we identified a mutant named *ms16600*, which exhibited a greatly reduced seed-setting rate. The mutant displayed normal vegetative growth, booting and heading (Fig. 1a), but partial panicle enclosure (Fig. 1b). The seed-setting rate was severely reduced compared to the wild type (WT) (Fig. 1b). The spikelets of the mutant looked normal externally (Fig. 1b), but the anthers within were smaller and pale yellow in color (Fig. 1c). I_2-KI staining showed that in >70% of the spikelets, the anthers failed to produce any normally stained pollen grains, and in <30% of the spikelets, the anthers produced a variable proportion of darkly stained pollen grains (Fig. 1d). Fluorescein Diacetate (FDA) staining indicated that the darkly stained pollen grains produced by the mutant emitted fluorescence similar to that of the WT (Additional file 1: Figure S1), indicating that they were viable pollen grains. When *ms16600* was cross-pollinated with HHZ, the seed setting rate was ~90% (Additional file 2: Table S1), which was equivalent to that of the control male sterile line Zhen18A (Chang et al. 2016a). These results indicated that the female fertility of the mutant was normal, and the reduced seed-setting rate was caused by defective pollen development.

Because some mutant spikelets produced a portion of normal pollen and were capable of setting seeds, we investigated whether the fertility of the mutant was affected by the environment. The mutants were grown in different seasons in Shenzhen to monitor the seed-setting rate. To prevent out-crossing, the mutant panicles were bagged. When the average temperature during the booting and heading stages was between 26 and 33 °C (with heading occurring in early August and early

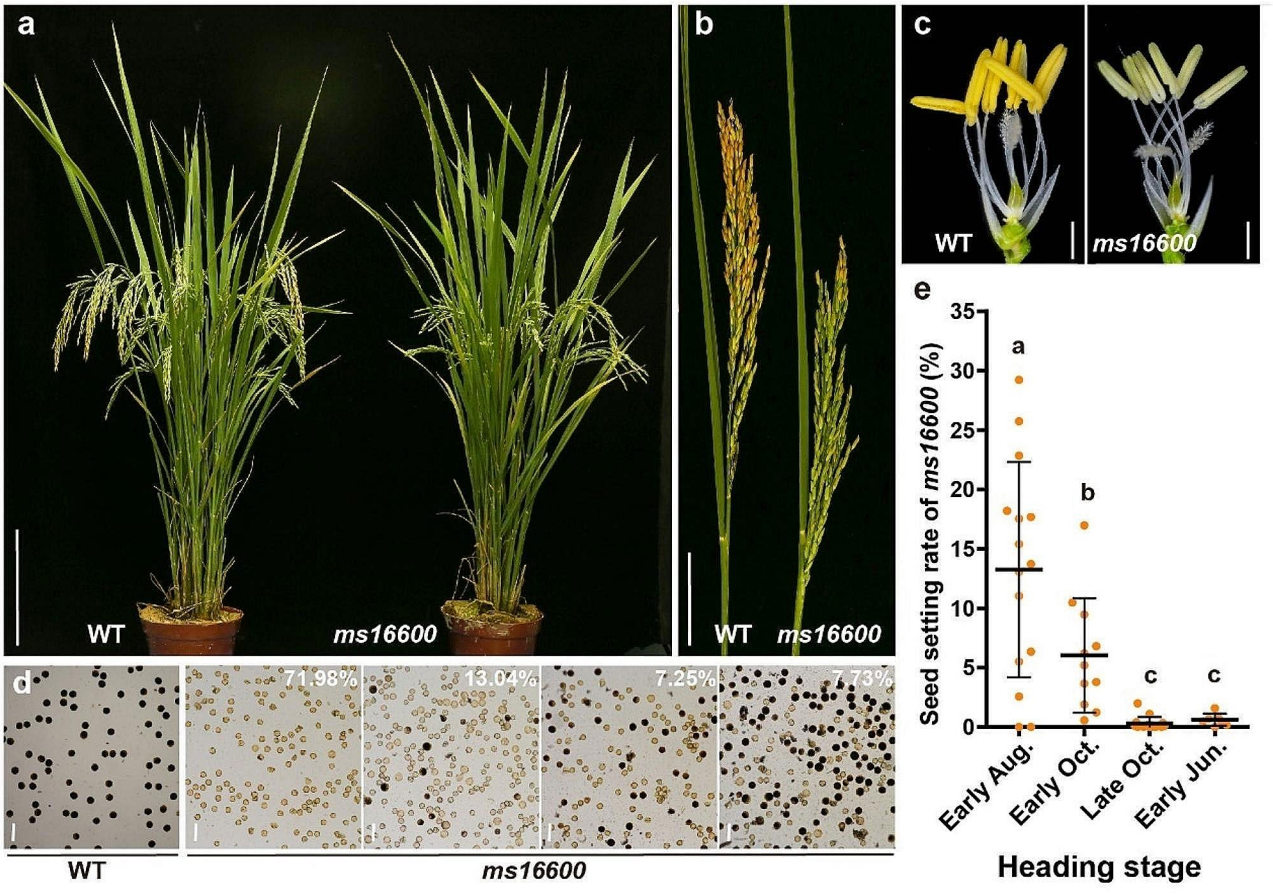

Fig. 1 Phenotypic characteristics of the *ms16600* mutant. **a** Plants of wild type (WT) and *ms16600* after heading. **b** Panicles from WT and *ms16600*. **c** Spikelets from WT and *ms16600*, with the palea and lemma removed. **d** Pollen grains from WT and *ms16600* stained with I_2-KI. A total of 207 *ms16600* spikelets were examined, and the number in each image represents the percentage of spikelets exhibiting the depicted phenotype. Scale bars = 20 cm (**a**); 5 cm (**b**); 2 mm (**c**); 100 μm (**d**). **e** Seed setting rates of *ms16600* heading at different seasons. The temperature range during the booting and heading stages in Shenzhen was 27–33°C for Early Aug. 2022, 26–33°C for Early Oct. 2022, 22–30°C for Late Oct. 2022, and 23–29°C for Early Jun. 2022, respectively. Different letters denote significant differences ($P < 0.01$, *t*-test); while identical letters indicate no significant difference

October), the average seed setting rate was between 6.02% and 13.26%, reaching a peak of 29.23%. In contrast, when the average temperature during these stages was between 22 and 26 °C (with heading in late October and early June), the mutant exhibited near-complete sterility (Fig. 1e). These results suggested that pollen development in *ms16600* mutant might be temperature-sensitive, and higher average temperatures could be favorable for pollen development in the *ms16600* mutant.

Histological Analysis of *ms16600* Mutant Anther

To elucidate the impact of the OsSNDP4 mutation on pollen development, we compared the anther developmental processes between the WT and *ms16600* mutant with microscopic analyses. In rice, anther development is divided into 14 stages based on morphological characteristics (Zhang et al. 2011). Transverse sections revealed no obvious difference between the WT and *ms16600* mutant before the tetrad formation (stage 8b) (Fig. 2a–d).

By stage 9, the tapetal cells in both the WT and *ms16600* mutant became thinner (Fig. 2e and f). The WT tapetal cell cytoplasm was highly condensed with the vacuoles almost completely disappeared (Figs. 2e and 3a), while the Ubisch bodies, which are thought to export sporopollenin precursors from the tapetum to the microspore, were generated on the outer surface of the tapetal cells (Fig. 3a). In contrast, in *ms16600* mutant, the tapetal cell cytoplasm was less condensed with many vacuoles visible inside (Figs. 2f and 3b), and the Ubisch bodies were not clearly visible (Fig. 3b). At this stage,

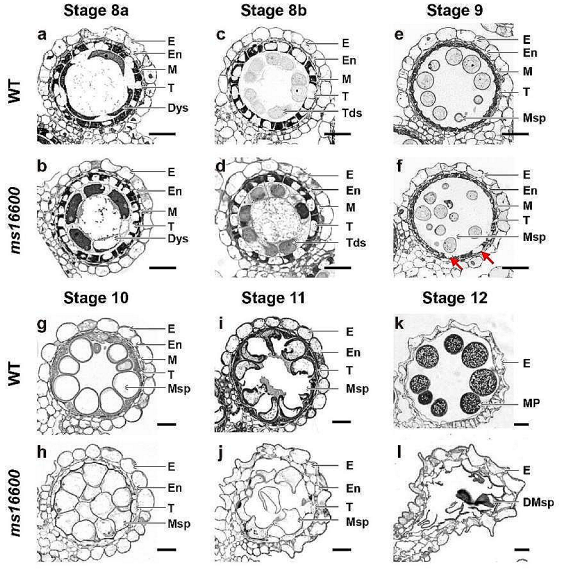

Fig. 2 Transverse sections of anther in wild type and *ms16600* from stage 8a to stage 12. Dys, dyads; DMsp, degenerated microspores; E, epidermis; En, endothecium; M, middle layer; MP, mature pollen; Msp, microspores; T, tapetum; Tds, tetrads. Red arrows in **f** show vacuoles within the tapetal cells. Scale bars = 20 μm

the callose wall surrounding microspores was degraded, and the released microspores were loosely arranged in a circle along the tapetum in the WT (Fig. 2e), with proexine deposited on the microspore surface (Fig. 3a). In *ms16600* mutant, microspores were also released from the tetrad but were scattered within the anther locule (Fig. 2f), and the proexine was thinner than that of the WT (Fig. 3b).

By stage 10, the WT tapetal cells further degenerated, yet the dense cellular contents were still visible (Figs. 2g and 3c), and the Ubisch bodies further enlarged in size and were tightly arranged on the tapetal surface (Fig. 3c, i). In *ms16600* mutant, tapetal cells contained much less cellular contents (Figs. 2h and 3d), and the Ubisch bodies were poorly developed (Fig. 3d, j). Meanwhile, spherical microspores were closely arranged along the tapetum in the WT, and their volume increased significantly with a large vacuole in the center and cytoplasm and nucleus moving to the cell edge (Fig. 2g), and the wall of microspores became obviously thickened (Fig. 3c). However, in *ms16600* mutant, the microspores were excessively enlarged due to the abnormally enlarged vacuole, and they squeezed each other in the anther locule, resulting in an irregular cell shape (Fig. 2h). The pollen exine was thinner compared with that of the WT (Fig. 3d).

By stage 11, the WT tapetum almost completely degenerated (Figs. 2i and 3e), and the Ubisch bodies enlarged further (Fig. 3e). Conversely, the mutant tapetal cells remained large with little cellular content inside (Figs. 2j and 3f), and they exhibited irregular Ubisch bodies (Fig. 3f). Meanwhile, the WT microspores became falcate with further thickened exine (Figs. 2i and 3e). The mutant microspores began to collapse with a decrease in cell volume and an irregular cell shape (Fig. 2j), and the pollen exine remained thinner than that of the WT (Fig. 3f).

By stage 12, the WT microspores developed into spherical pollen grains filled with numerous starch granules and dense cellular contents (Figs. 2k and 3m), and only the epidermis layer remained visible in the WT anther wall (Fig. 2k). In contrast, the mutant microspores completely collapsed, leaving only the irregularly shaped pollen wall (Figs. 2l and 3n). Both the epidermis and tapetum layers were clearly visible in the mutant anther wall (Fig. 2l). The cuticle on the outer surface of the anthers did not show a significant difference between the WT and *ms16600* mutant (Fig. 3g–h, k–l).

Identification of the Causal Mutation for *ms16600* Mutant

We employed the *s*imultaneous *i*dentification of *m*ultiple causal *m*utations (SIMM) method described by Yan et al. (2017) to determine the causal mutation in the *ms16600* mutant. Initially, the mutant was crossed with the wild-type HHZ. The resulting F_1 plants all showed normal seed-setting rates. Self-pollination of the F_1 plants

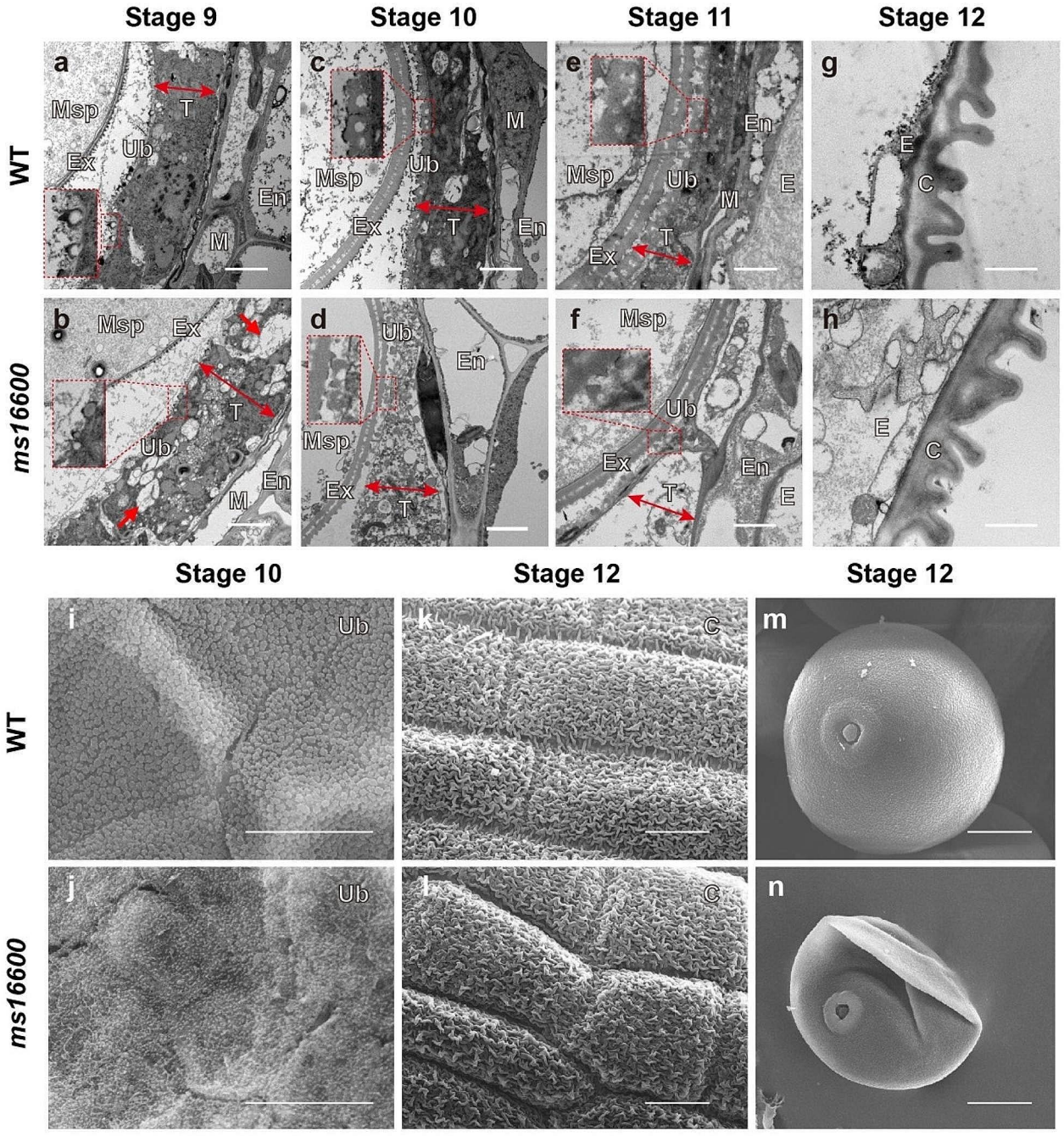

Fig. 3 Electron microscope analysis of the wild type and *ms16600* anthers from stage 9 to stage 12. **a**–**h**, transmission electron microscopy results; **i**–**n**, scanning electron microscopy results. C, anther surface cuticle; E, epidermis; En, endothecium; Ex, exine; M, middle layer; Msp, microspores; T, tapetum; Ub, Ubisch body. Ubisch bodies outlined in the dashed boxes in **a** to **h** are enlarged for clarity. The tapetal cell is indicated by red double-headed arrows. Red arrows in **b** show vacuoles within the tapetal cells. Scale bars = 2 μm (**a**–**h**); 10 μm (**i**–**n**)

yielded an F_2 population that segregated approximately in a 3:1 ratio of normal to reduced fertility (Additional file 3: Table S2), indicating that the mutant phenotype was due to a single recessive mutation.

Thirty plants of low seed-setting rates were selected from the F_2 segregating population for DNA extraction. Equal amount of genomic DNA extracted from these 30 individuals was pooled and bulk-sequenced to a depth of ~ 30 × coverage of the rice genome. After removing linker sequence and the sequences of low quality or low coverage, the high-quality sequence data were aligned against the Nipponbare reference genome and compared with

the re-sequencing data from other HHZ EMS mutants for identification of EMS-induced mutation sites in *ms16600* using the SIMM pipeline. SNP index and Euclidean distance (ED^6) was calculated for each SNP site. The SNP site with the highest scores for both SNP index and ED^6 was considered the candidate mutation site associated with the mutant phenotype (Yan et al. 2017).

A candidate mutation site was identified at the end of chromosome 2 (Fig. 4a). This mutation is situated in exon 10 of the gene *LOC_Os02g04020*, where the codon TGT (encoding amino acid Cys351) was changed to TGA, leading to premature termination of the protein (Fig. 4b). To establish the linkage between this mutation and the phenotype, a high-resolution melting (HRM) assay was performed on a F_2 segregation population. Among the 1917 F_2 progeny genotyped, those with homozygous wild-type (T/T) or heterozygous (T/A) genotypes exhibited normal fertility, whereas those with homozygous mutant genotype (A/A) showed reduced seed-setting rates (Additional file 4: Table S3). This indicates that the T to A mutation was tightly linked with the mutant phenotype.

To confirm the function of the mutant gene, we conducted CRISPR knockout of the *LOC_Os02g04020* gene in HHZ. To enhance the likelihood of successful gene editing, we designed four target sites (Target 2, Target 3, Target 5, and Target 9) within the second, third, fifth and ninth exons of the target gene, respectively, and constructed a multi-target editing vector (CR2359) for transformation into wild-type HHZ. Ten independent knockout lines (*Cr-1* to *Cr-10*) were obtained, all exhibiting small insertions or deletions at the target sites (Additional file 5: Table S4). To exclude the CRISPR T-DNA from the genome, T_0 plants were crossed with wild-type HHZ, and homozygous knockout mutants devoid of T-DNA were isolated from the F_2 progeny for subsequent phenotype analysis. These homozygous knockout mutants displayed phenotypes similar to the *ms16600* mutant, including small, pale anthers, pollen abortion, and reduced seed-setting rates (Fig. 4c–k, Additional file 6: Figure S2, Additional file 5: Table S4).

To further validate the function of the mutant gene, we conducted a gene complementation experiment. A genomic fragment encompassing the *LOC_Os02g04020* gene, along with a 3121 bp promoter region upstream of the start codon ATG, and an 896 bp fragment downstream of the stop codon TGA (Fig. 4b), was cloned into a binary vector and introduced into the *ms16600* mutant. Two independent transgenic lines, *Com-1* and *Com-2*, were obtained, both of which exhibited high seed-setting rates upon self-pollination. The offspring derived from self-pollination carrying the transgene (*Com-1P* and *Com-2P*) exhibited normal seed-setting, normal anthers, and normal pollen, while those lacking the transgene exhibited a phenotype similar to the *ms16600* mutant (Fig. 4l–q, Additional file 6: Figure S2). Moreover, crossing the transgene into the CRISPR knockout mutant lines restored the seed-setting rate of the homozygous CRISPR mutant to normal (Additional file 6: Figure S2, Additional file 7: Table S5). The above results confirm that the phenotype of *ms16600* is due to the loss of function of *LOC_Os02g04020*.

Phylogenetic Analysis of OsSNDP4

LOC_Os02g04020 encodes the Sec14 Nodulin Domain Containing Protein 4 (OsSNDP4) (Huang et al. 2016a). Conserved domain analysis indicated that OsSNDP4 possesses a conserved N-terminal Sec14 domain and a C-terminal plant-specific nodulin domain (Additional file 8: Figure S3a). The mutation in *ms16600* introduces a termination codon at the end of the Sec14 domain, resulting in a truncated protein that contains almost a complete Sec14 domain but lacks the nodulin domain (Additional file 8: Figure S3a).

Proteins containing the Sec14 domain are ubiquitous in eukaryotic cells. The yeast Sec14 protein is the prototype of this protein family (Montag et al. 2023). Sec14 can bind simultaneously to a PC and a PI molecule and promotes the phosphorylation of PI by PI 4-OH kinase (Schaaf et al. 2008). Sec14 facilitates lipid transport from ER to Golgi in yeast cells and can transfer PI and PC molecules between membranes in vitro (Bankaitis et al. 1989, 1990; Schaaf et al. 2008). A search of the Arabidopsis and rice genomes revealed 32 and 27 Sec14 domain-containing proteins, respectively (Huang et al. 2016a). These include 13 Arabidopsis and 13 rice proteins that possess only the Sec14 domain; 6 Arabidopsis and 4 rice proteins that contain both the Sec14 and GOLD domains, and 13 Arabidopsis and 10 rice proteins that harbor the Sec14 and nodulin domains (Ghosh et al. 2015; Huang et al. 2016a).

Proteins containing both a Sec14 domain and a nodulin domain are referred to as AtSFHs in Arabidopsis and OsSNDPs in rice (Huang et al. 2016a). The Sec14 domains of these proteins are highly conserved and possess conserved amino acid residues for PI binding (referred to as the PI-binding barcode) and PC-binding (referred to as the PC-binding barcode), as observed in yeast Sec14 protein (Additional file 8: Figure S3b). The Sec14 domains from several proteins, including AtSFH1, AtSFH4, AtSFH5, AtSFH9, and OsSNDP1, all exhibit in vitro PI binding and transfer activities as well as PI 4-OH kinase stimulating activities, and both activities depend on the conserved barcode amino acid residues (Huang et al. 2016b). Previous studies have showed that the functions of Sec14-nodulin family proteins AtSFH1 and AtSFH5 depend not only on the Sec14 domain but also on the nodulin domain (Ghosh et al. 2015; Yao et al.

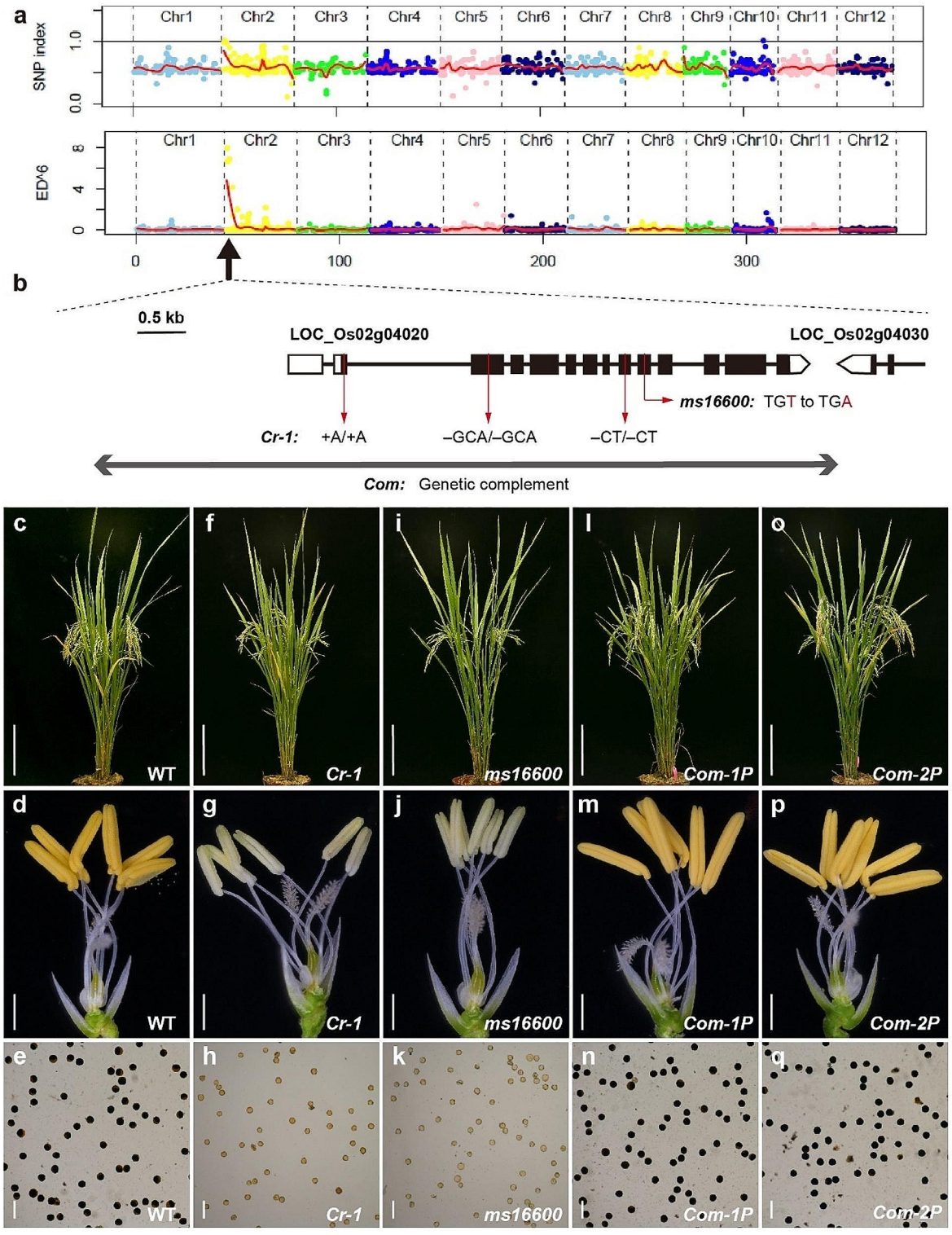

Fig. 4 Identification and verification of the mutant gene through CRISPR knockout and transgenic complementation. **a** Identification of the causal mutation site using SIMM method. The SNP index and Euclidean distance (ED) scores of EMS-induced SNPs are depicted as dots. **b** Gene structure of *LOC_Os02g04020*. The mutation site in *ms16600* (TGT to TGA) and the mutation sites in *Cr-1* (+A/+A, –GCA/–GCA, –CT/–CT) are shown. Black boxes represent exons, white boxes represent UTRs, and the lines between them denote introns. The line with two arrows indicates the genomic fragment used for transgenic complementation. **c**–**e** Wild type HHZ. **f**–**h** CRISPR knockout mutant *Cr-1*. **i**–**k** *ms16600* mutant. **l**–**n** Transgenic complementation plant *Com-1P*. **o**–**q** Transgenic complementation plant *Com-2P*. Scale bars = 20 cm (**c**, **f**, **i**, **l**, **o**); 1 mm (**d**, **g**, **j**, **m**, **p**); 100 μm (**e**, **h**, **k**, **n**, **q**)

2023). Based on the sequence characteristics of the C-terminal nodulin domains, the 10 rice OsSNDPs and the 14 Arabidopsis AtSFHs are classified into three groups (Additional file 9: Figure S4a). Class I nodulins are characterized by an uninterrupted stretch of seven or more basic residues with adjacent aromatic residues (Additional file 9: Figure S4b). The class I nodulin domain of AtSFH1 has been demonstrated with the PI(4,5)P_2 binding activity (Ghosh et al. 2015). Class II nodulins exhibit C-terminal 6–8 basic residues and a penultimate Cys residue, but the uninterrupted stretch of basic residues in Class II is shorter than those in Class I nodulin domains (Additional file 9: Figure S4b). Class III nodulin C-termini have 8–12 basic residues, but the sequences are more divergent (Additional file 9: Figure S4b). OsSNDP4 falls into Class II according to phylogenetic analysis (Additional file 9: Figure S4a). The class II nodulin domain of AtSFH5 does not bind lipid on its own, but is required for maintaining the overall structure of the full-length AtSFH5 protein (Yao et al. 2023). The AtSFH5 protein shows strong binding to phosphatidic acid (PA) and relatively weaker binding towards PI(3,4)P_2, PI(3,5)P_2, PI(4,5)P_2, PI(3,4,5)P_3, and PI(4)P in a protein-lipid overlay assay (Yao et al. 2023).

OsSNDP4 Gene Expression and Subcellular Localization of OsSNDP4 Protein

The *ms16600* mutant exhibited abnormal anther development but no obvious defects in other organs. To understand the dedicated role of *OsSNDP4*, we analyzed the spatial and temporal gene expression patterns of *OsSNDP4* using quantitative reverse transcription-PCR (qRT-PCR). As shown in Fig. 5a, *OsSNDP4* expression was detected in all tested tissues, including roots, culms, leaves, glumes, pistils and anthers. Notably, the expression levels were significantly higher in stage 10–12 anthers than in other tissues, correlating with the observation that *ms16600* mutant exhibited clear defects in anthers after stage 9. The mutation in *ms16600* significantly reduced the transcript level of the mutant gene (Fig. 5b).

As mentioned above, the *ms16600* mutant exhibited different seed setting rates when grown in different seasons, suggesting that *OsSNDP4* might be regulated by temperature. To investigate this, we subjected rice plants to cold treatment (6 °C) and accessed the gene expression of *OsSNDP4*. As shown in Additional file 10: Figure S5, the transcripts of *OsSNDP4* were induced following exposure to low temperatures.

The subcellular localization of proteins is crucial to their proper function. Analyses using TargetP, SignalP, and Cell-Ploc failed to identify a secretion signal peptide, mitochondria or chloroplast localization signal, or an endoplasmic reticulum (ER) retaining signal in the OsSNDP4 protein sequence. However, ScanProsite predicted the presence of a CRAL-TRIO lipid binding domain between amino acids 150 and 324 and a bipartite nuclear localization signal (NLS) between amino acids 45 and 61 (Additional file 11: Figure S6). Additionally, cNLS Mapper also identified nuclear localization signals within this region (Additional file 11: Figure S6). To ascertain the subcellular localization of the OsSNDP4 protein, we generated a recombinant OsSNDP4-EGFP fusion protein by appending EGFP to the C-terminus of OsSNDP4. Expression of this fusion protein in rice protoplasts showed a strong green fluorescence signal in the nucleus and associated with the ER (Fig. 5c). In addition, green fluorescence signal was also detected along the vacuole membrane (Fig. 5c). The observation of OsSNDP4 localization signals associated with the ER and surrounding the vacuoles is consistent with the proposed role of Sec14 family proteins in binding with phosphoinositides.

OsSNDP4 Demonstrates Significant Binding to PI(3)P

Several Sec14 domain containing proteins, with or without the additional domains, have been shown to bind PI, PIPs, and other lipid molecules with varying specificities (Ghosh et al. 2015; Huang et al. 2016a; Yao et al. 2023). To assess the lipid binding capability of OsSNDP4, the recombinant MBP-OsSNDP4 protein was expressed in *E. coli* and purified using MBP-binding beads. A protein-lipid overlay assay was conducted with the purified MBP-OsSNDP4 fusion protein, using purified MBP and PI(4,5)P_2 Grip [specific for PI(4,5)P_2] as negative and positive controls. As anticipated, MBP alone did not exhibit binding to any lipids, while PI(4,5)P_2 Grip showed strong binding to PI(4,5)P_2. The OsSNDP4 protein showed strong binding to PI(3)P, weaker binding to PA, and no binding to other lipids tested (Fig. 6). We also tested whether the separated Sec14 domain and nodulin domain of OsSNDP4 were capable of lipid binding. Both domains showed minimal binding to PI(3)P compared to the full-length OsSNDP4 protein (Fig. 6).

Influence of *OsSNDP4* Mutation on the Expression of Genes in Anther

Histological examination of anther development revealed that the WT and *ms16600* mutant began to exhibit phenotypic difference in anthers at stage 9. To elucidate the molecular mechanisms by which OsSNDP4 regulates pollen development, we performed RNA-seq analysis to compare the gene expression profiles between WT and *ms16600* mutant anthers at stage 9. Using a cut-off of >2-fold change and a *P*-value<0.05, we identified a total of 5561 differentially expressed genes (DEGs), with 2715 genes up-regulated and 2846 genes down-regulated in the mutant anthers (Additional file 12: Table S6, Additional file 13: Table S7). The DEGs include at

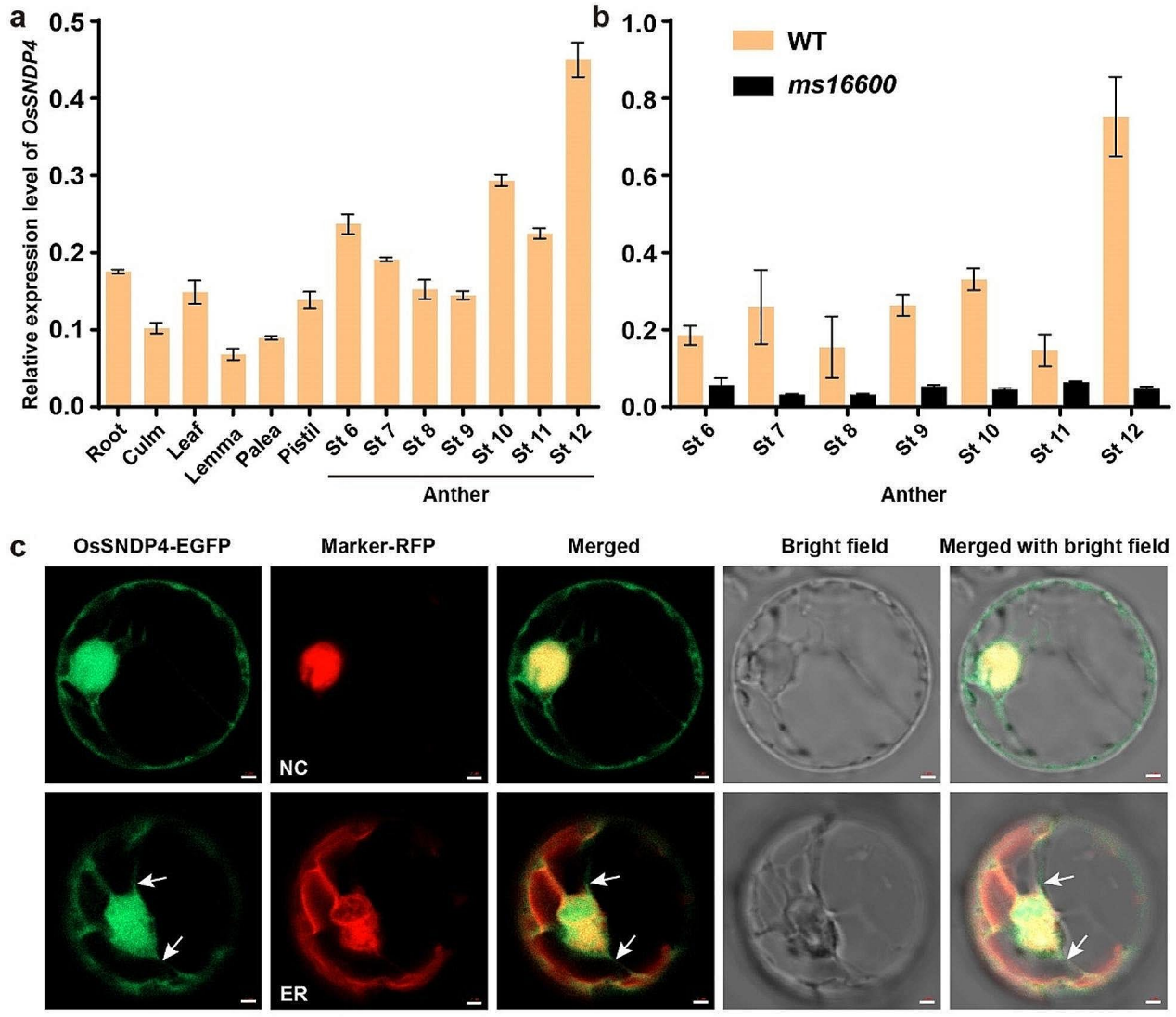

Fig. 5 *OsSNDP4* gene expression and subcellular localization of the OsSNDP4 protein. **a** Expression profile of the *OsSNDP4* gene in various tissues. **b** Comparison of *OsSNDP4* transcript levels between the wild type HHZ and the *ms16600* mutant during anther development, from stage 6 to stage 12. Pistils and other tissues were harvested from plants at the heading stage. **c** Subcellular localization of the OsSNDP4 protein in rice protoplasts. NC and ER denote the nuclear marker ARF19IV-mCherry and the endoplasmic reticulum marker RFP-HDEL, respectively. Arrows point to the vacuole membrane

least 61 genes that are known to be crucial for rice pollen development (Additional file 14: Table S8). It is striking that 59 of these 61 genes were down-regulated in the *ms16600* mutant anthers (Additional file 14: Table S8). To validate the RNA-seq results, we selected six DEGs (*CYP703A3*, *TDR*, *DPW*, *CYP704B2*, *PAIR2*, and *OsC4*) that are important for pollen development and assessed their expression during anther development via qRT-PCR (Additional file 15: Figure S7). The expression of all these genes were consistent with the RNA-seq findings, confirming the reliability of the RNA-seq analysis. KEGG pathway analysis of the DEGs indicated that genes involved in ribosome biogenesis, the biosynthesis of flavonovid and other secondary metabolites, and transporters were up-regulated in the *ms16600* mutant anthers. Conversely, genes related to sporopollenin synthesis, including those involved in fatty acid biosynthesis and lipid metabolism, the biosynthesis of secondary metabolites such as phenylpropanoid and terpenoid, the biosynthesis of lipid polymers, and signaling proteins and transcription factors, were down-regulated in the *ms16600* mutant anthers (Additional file 16: Figure S8). Interestingly, an enrichment of exosome proteins was also observed among the down-regulated genes in *ms16600* mutant anthers, suggesting that OsSNDP4 may play a role in regulating protein exocytosis.

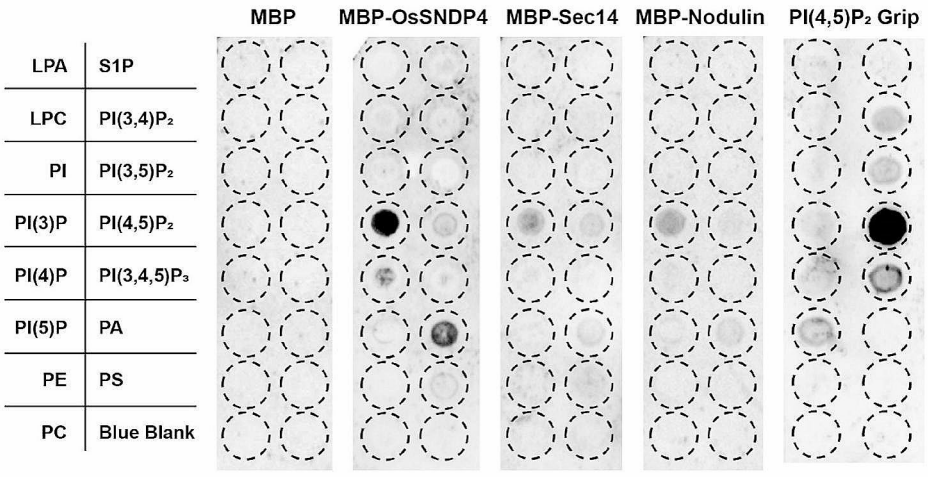

Fig. 6 Protein-lipid blot overlay assay assessing the lipid binding and specificity of OsSNDP4. Recombinant proteins MBP-OsSNDP4, MBP-Sec14, and MBP-Nodulin were purified from *E. coli*. MBP alone and PI(4,5)P_2 Grip were used as control. The left panel of the figure provides a schematic representation of the lipids present on the strip, including lysophospharidic acid (LPA), lysophosphacholine (LPC), phosphatidylinositol (PI), PI 3-phosphate [PI(3)P], PI 4-phosphate [PI(4)P], PI 5-phosphate [PI(5)P], phosphatidylethanolamine (PE), phosphatidylcholine (PC), sphingosine 1-phosphate (S1P), PI 3,4-bisphosphate [PI(3,4)P_2], PI 3,5-bisphosphate [PI(3,5)P_2], PI 4,5-bisphosphate [PI(4,5)P_2], PI 3,4,5-trisphosphate [PI(3,4,5)P_3], phosphatidic acid (PA), phosphatidylserine (PS), and a blue blank control

Discussion

By characterizing the *ms16600* mutant, we found that *OsSNDP4* is important for the development of rice pollen. *OsSNDP4* encodes a Sec14-nodulin domain protein that demonstrates affinity for binding to PI(3)P, as evidenced by the protein-lipid overlay assay. *OsSNDP4* is expressed in all tested vegetative and floral organs, with a relatively higher expression level in the anthers during pollen exine development (Fig. 5a). Sec14 was identified in yeast as a cytosolic factor required for transport of secretory proteins from the Golgi complex (Bankaitis et al. 1989). It is a PC/PI transfer protein capable of exchanging the phospholipids between membranes in vitro (Bankaitis et al. 1990). Sec14 can bind PC and PI simultaneously and catalyze the synthesis of PI(4)P by presenting PI to PI 4-OH kinases (Schaaf et al. 2008). These findings lead the proposal that Sec14 executes its function by creating a lipid environment crucial for the biogenesis of secretory vesicles from the Golgi network (Mousley et al. 2012). Crystal structure analysis of Sec14 and its yeast homologue Sfh1 revealed the critical amino acid residues for PI and PC binding (Schaaf et al. 2008). These residues are highly conserved in Sec14-nodulin proteins (Huang et al. 2016a). Importantly, a few Sec14-like domains, including those from AtSFH1, AtSFH4, AtSFH5, AtSFH9, and OsSNDP1, which possess the conserved lipid-binding residues, all exhibit in vitro PI and PC transfer activities as well as PI 4-OH kinase stimulating activities, and both activities depend on the conserved amino acid residues (Huang et al. 2016b). Sequence comparison indicated that OsSNDP4 also has the conserved Sec14 domain as well as the important lipid binding residues (Additional file 8: Figure S3), which is consistent with the finding that OsSNDP4 can bind PI(3)P.

Genetic analysis indicated that *OsSNDP4* regulates pollen fertility as a sporophytic factor in Mendelian inheritance. Consistent with this result, *ossndp4* mutant plant exhibited abnormal tapetal cell degradation, defective Ubisch body formation, a much thinner pollen exine, and pollen abortion (Figs. 2 and 3). The molecular genetic behaviors of *OsSNDP4* differ from those of *OsSNDP3*, a paralog of *OsSNDP4* that is also required for pollen fertility (Moon et al. 2022). *OsSNDP3* is specifically expressed in mature pollen. When *OsSNDP3*/*ossndp3* was used as pollen donor, the mutant gene could not be transmitted to the next generation (Moon et al. 2022), indicating that *OsSNDP3* acts as a gametophytic gene in regulating pollen fertility. OsSNDP3 contains a Sec14 domain and a type I nodulin domain (Additional file 9: Figure S4). Similar to AtSFH1/COW1 and OsSNDP1, two other proteins with a Sec14 domain and a type I nodulin domain, OsSNDP3 was found to co-localize with PI(4,5)P_2 (Moon et al. 2022), a phosphoinositide associated with the plasma membrane and crucial for plasma membrane polarity (Lebecq et al. 2022). AtSFH1/COW1 and OsSNDP1 are essential for root hair elongation (Böhme et al. 2004; Vincent et al. 2005; Huang et al. 2013b), whereas OsSNDP3 is crucial for pollen tube growth (Moon et al. 2022). OsSNDP3 interacts with OsSNDP2, another protein with a Sec14 domain and a type I nodulin domain that is also highly expressed in mature pollen but plays a minor role in regulating pollen tube growth (Moon et al. 2022). The differences in genetic behaviors, gene expression patterns, and substrate binding specificities indicate

that OsSNDP4 and OsSNDP3/OsSNDP2 regulate rice male fertility through distinct mechanisms.

In plant, PI(3)P is primarily generated by PI 3-kinase (PI3K) that phosphorylates PI at the D-3 position (Welters et al. 1994; Lee et al. 2008). In Arabidopsis, PI3K is encoded by the single-copy gene *AtVPS34*, which is crucial for normal plant development (Welters et al. 1994). The plant PI3K protein is associated with active nuclear and nucleolar transcription sites (Bunney et al. 2000). Consistent with the nuclear localization of the PI(3)P-synthesizing enzyme, OsSNDP4, which can bind PI(3)P, demonstrated a strong nuclear localization signal in the rice protoplast transient expression assay (Fig. 5c). RNA-seq analysis revealed significant enrichment of ribosome biogenesis genes that were up-regulated in the *ossndp4* mutant anther, implicating that the nuclear localized OsSNDP4 protein may play a role in regulating ribosome biogenesis, a process that occurs in the nucleus (Jiao et al. 2023).

Additionally, OsSNDP4-EGFP exhibited co-localization with the ER marker and a fluorescence signal surrounding the vacuole (Fig. 5c). Several studies have shown that PI(3)P is predominantly associated with highly motile structures such as the prevacuolar compartment, late endosome, and the tonoplast (Vermeer et al. 2006; Simon et al. 2014; Hammond and Balla 2015). These vesicles are all related to ER functions within the cell (Mousley et al. 2012). In yeast, PI(3)P is essential for vesicle-mediated delivery of vacuolar enzymes (Stack and Emr 1994), and in animal cells, inhibition of PI(3)P synthesis by chemical inhibitors disrupts protein targeting from the trans-Golgi network to the lysosomes (Brown et al. 1995; Davidson 1995). Similarly, tobacco suspension cells treated with chemicals interfering with PI(3)P synthesis failed to deliver proteins into vacuoles (Matsuoka et al. 1995). Furthermore, PI(3)P inhibitors induce swelling or vacuolation of the prevacuolar compartment (Tse et al. 2004) and block retrograde transport of vacuolar sorting receptors to the *trans*-Golgi network (daSilva et al. 2005). Overexpression of a PI(3)P binding protein inhibits trafficking of the vacuolar protein in Arabidopsis protoplasts (Kim et al. 2001). Through a protein-lipid overlay assay, we confirmed that OsSNDP4 exhibits a significant affinity for binding to PI(3)P (Fig. 6). Consistent with the role of PI(3)P in regulating vacuole dynamics, microscopic examination of the *ossndp4* mutant anthers revealed abnormal vacuole dynamics in both tapetal cells and microspores (Figs. 2 and 3). In wild-type tapetal cells, a large vacuole was present at stage 8 during meiosis, which became nearly invisible by stage 9. However, in the mutant tapetal cells, vacuoles were clearly visible under both semi-thin section and TEM observation by stage 9 (Figs. 2 and 3). At stage 10, the mononuclear microspores of the wild-type plant exhibited a large central vacuole, whereas in the mutant microspores, the vacuole was abnormally enlarged (Fig. 3). It appeared that the *ossndp4* mutant tapetal cells underwent earlier degradation of cellular contents and organelles compared to the wild-type (Fig. 2). Based on these observations, we hypothesized that OsSNDP4 may executes its function at least in part by binding PI(3)P, a lipid signal that regulates the behavior of the pre-vacuolar compartment and vacuoles.

Previous studies indicated that PI(3)P plays an important role in regulating pollen development. For instance, the Arabidopsis plants heterozygous for *AtVPS34/atvps34* were unable to transmit the mutant gene through the male gametophyte (Lee et al. 2008). Microscopic analysis revealed that many mature pollen grains from the *AtVPS34/atvps34* heterozygous plants contained large vacuoles even at the mature pollen stage, whereas pollen from wild-type plants exhibited many small vacuoles starting from the vacuolated pollen stage (Lee et al. 2008). PI(3)P can be converted into PI(3,5)P_2 by PI(3)P 5-kinases (Whitley et al. 2009). In Arabidopsis, there are four genes, FAB1a, FAB1b, FAB1c, and FAB1d, encoding PI(3)P 5-kinases (Whitley et al. 2009). Microspore carrying double mutation of *FAB1a* and *FAB1b* displayed severe defects in vacuolar reorganization following the first mitotic division and abnormally large vacuoles in pollen at the tricellular stage, leading to the collapse of the majority of pollen grains carrying both mutant alleles (Whitley et al. 2009). These findings suggest that the homeostasis of PI(3)P and PI(3,5)P_2 is important in modulating the dynamics of vacuolar rearrangement essential for successful pollen development.

The presence of abnormally enlarged vacuole was also observed in microspores of the *ossndp4* mutant at stage 10. This observation aligns with the hypothesis that OsSNDP4, as a PI(3)P-binding protein, in involved in regulating vacuole dynamics in pollen. Genetic data indicated that OsSNDP4/*ossndp4* heterozygous plants transmitted the mutant gene normally to the next generation, suggesting that the *ossndp4* mutation, when present in the haploid genome, has a minor impact on pollen fertility. Given that defective pollen was only observed in the homozygous *ossndp4* mutant plant, we speculate that the OsSNDP4 protein contributed by the tapetum and the pollen mother cell plays a significant role in regulating vacuole dynamics in microspores.

Conclusions

In summary, this study demonstrated that OsSNDP4, a PI(3)P-binding protein with a Sec14-nodulin domain, is indispensable for pollen development and male fertility in rice. The mutation of *OsSNDP4* led to abnormal vacuole behavior in tapetal cells and microspores, abnormal degradation of tapetal cells, inhibition of Ubisch body formation, reduced expression of genes involved in

sporopollenin biosynthesis, and abnormal exine formation. Based on the lipid-binding specificity of OsSNDP4 with PI(3)P and the cellular and molecular defects exhibited by the *ossndp4* mutant anther, we propose that *OsSNDP4* regulates pollen development by binding PI(3)P and regulating the dynamics of membrane systems, and the alterations in the dynamics of membrane systems are likely to influence the expression of genes crucial for sporopollenin biosynthesis and exine formation.

Methods

Plant Material and Growth Conditions

The *ms16600* mutant was identified from a mutant library created using EMS-treated *indica* rice variety HHZ (Chen et al. 2014). The *ms16600* mutant was crossed with the WT HHZ to generate the F_1 generation, which were then self-pollinated to produce the F_2 population. The F_2 plants were utilized for phenotypic characterization, genetic analysis, mapping of the mutant gene, and for genetic complementation experiments. All plant materials were cultivated in a paddy field in Shenzhen from March to November.

Morphological Analysis of the Mutant

Plants at the heading stage were used for morphological examination of floral organs and for pollen staining. The seed setting rates were assessed in plants at the yellow ripe stage. Photographs of the plants and panicles were captured using a Canon EOS 5D digital camera, while images of the spikelet and pollen were taken with a Nikon AZ100 microscope. For pollen fertility analysis, mature anthers prior to flowering were crushed in 1% I_2-KI or 50 μg/mL FDA (diluted in an 8% sucrose solution) to release the pollen grains. Fertile pollen grains typically stain darkly with I_2-KI and emit fluorescence (excited at 488 nm and detected at 530 nm) following FDA staining, whereas abortive pollen grains exhibit a lighter staining and do not fluoresce. To evaluate female fertility, the *ms16600* mutant was hand-pollinated with WT HHZ pollen, using the male sterile line Zhen18A as a control (Chang et al. 2016a). To determine the seed setting rates, an average was calculated from 10 individual plants per genotype, with three representative panicles sampled from each plant. Temperature data for Shenzhen can be accessed through the local weather website (https://lishi.tianqi.com/shenzhen/).

Microscopic Analysis of the Mutant

Anthers from both WT and *ms16600* mutant plants at stages 8 to 12 were sampled according to the standards described in Zhang et al. (2011). The microscopy procedures detailed by Chang et al. (2016b) were followed for this study. Anthers were fixed using a 0.1 M PBS solution containing 2.5% glutaraldehyde and 2% paraformaldehyde, which was followed by resin embedding, semi-thin sectioning, ultra-thin sectioning, and subsequent examination under a light microscope and transmission electron microscopy (TEM). Prior to scanning electron microscopy (SEM) observation, the anthers were fixed in 70% FAA (comprising 5 mL of 38% formaldehyde, 5 mL of acetic acid, and 90 mL of 70% alcohol). For each pair of comparison, anthers from multiple spikelets of the same developmental stages were analyzed through semi-thin sections to ensure that the anthers were at the same developmental stages.

Mapping and Confirmation of Linkage for the Mutant Gene

Thirty plants with seed-setting rate < 5% were chosen from the F_2 population derived from the cross between the *ms16600* mutant and HHZ. Genomic DNA was extracted from each of these individuals and equally mixed for sequencing using the Illumina Hiseq 2000 platform. The sequence data were analyzed computationally with the SIMM method, as described by Yan et al. (2017). Co-segregation of the candidate mutation with the phenotype in F_2 population was analyzed using HRM analysis on the LightScanner 96 instrument (Idaho, USA) (Lochlainn et al. 2011). The primer pair ms16600-T_A-64-HRM-F and ms16600-T_A-64-HRM-R used for the HRM assay is provided in Additional file 17: Table S9.

Construction of Gene Knockout and Genetic Complementation Vectors and Identification of Transgenic Plants

CRISPR/Cas9 mediated gene knockout was employed to generate additional mutant alleles. Target sites within the second, third, fifth and ninth exons of the *OsSNDP4* gene (*LOC_Os02g04020*) were determined using the CRISPR-P v2.0 online tool and designated as Target 2, Target 3, Target 5, and Target 9, respectively. The target site sequences were cloned into the pYLCRISPR-MH vector as described by Ma et al. (2015), resulting in the multi-target editing vector CR2359. Following sequence verification, this vector was introduced into the *Agrobacterium tumefaciens* AGL0 strain for transformation into HHZ. To identify mutations in the T_0 plants, a primer pair specific to each target site was used to amplify the target segment for sequencing. Based on the sequencing results, HRM primers were designed for genotyping the T_1 progeny. The primers for CR2359 vector construction, target site sequencing, and HRM analysis are listed in Additional file 17: Table S9.

For transgenic complementation, an 8361 bp genomic fragment of *OsSNDP4*, encompassing a 3121 bp promoter region upstream of the ATG start codon and an 896 bp region downstream of the TGA stop codon, was PCR-amplified using the ms16600-gDNA-Com-F and ms16600-gDNA-Com-R primer pair with HHZ genomic

DNA as the template. The PCR product was cloned into the binary vector pCAMBIA1300 to create the Com vector. After sequence confirmation, this vector was introduced into the *Agrobacterium tumefaciens* AGL0 strain for transgenic complementation. Two primer pairs,1300-YJ-F and Com16600-YJ-R, and Com16600-YJ-F and 1300-YJ-R, were used for identification of positive T_0 transgenic plants. To determine the genomic background of the transgenic plant, a two-round PCR approach was employed to genotype the *OsSNDP4* mutation site. The primers Com16600-BJgDNA-F and Com16600-BJgDNA-R were used in the first round of PCR to amplify the genome DNA fragment. Subsequently, the PCR products were used as templates for genotyping by HRM, utilizing the ms16600-T_A-64-HRM-F and ms16600-T_A-64-HRM-R primer pair. All the primers are detailed in Additional file 17: Table S9.

Protein Alignment and Phylogenetic Analysis

The OsSNDP4 protein sequence was used as a query in Smart-BLAST on NCBI to identify the 14 Arabidopsis and 9 rice proteins with the highest sequence similarity. These proteins were aligned using ClustalW with its default settings, and a phylogenetic tree was generated using the maximum likelihood method in MEGA-X (Kumar et al. 2018).

Gene Expression Analysis

Anthers at various developmental stages were collected from the wild-type HHZ according to the standard described in Zhang et al. (2011). Roots, culms, flag leaves, lemmas, paleas and pistils were collected at the flowering stage. Each sample comprised at least three biological replicates. The procedures described by Chang et al. (2018) were used for the total RNA extraction, reverse transcription, and quantitative PCR, with primers shown in Additional file 17: Table S9. qRT-PCR was carried out on an Applied Biosystems 7500 Real-Time PCR System. Each experiment was conducted three times, with three technical replicates per run. *OsUbiquitin* was employed as the internal control for normalization. Relative expression levels were measured using the $2^{-\Delta Ct}$ analysis method. The primers for qRT-PCR analysis are listed in Additional file 17: Table S9.

Subcellular Localization Analysis

The 1872-bp CDS of the *OsSNDP4* gene (excluding the stop codon) was amplified using the wild-type HHZ anther cDNA as a template and the OsSNDP4-EGFP-F and OsSNDP4-EGFP-R primer pair. The PCR product was then ligated upstream of the *EGFP* in the pAN580 vector to create the subcellular localization vector OsSNDP4-EGFP. After sequencing verification, high-quality plasmid was purified using the HiPure Plasmid Mini Kit (Magen Biotechnology, China) and transformed into rice protoplasts along with the ER marker RFP-HDEL (Virgili-López et al. 2013) and the nuclear marker ARF19IV-mCherry (Zhai et al. 2014). The protocol for preparing rice protoplasts and the PEG-mediated transformation was based on the method described by Chen et al. (2006). The transformed protoplasts were observed under a laser confocal microscope (Carl Zeiss LSM-800).

Protein Lipid Overlay Assay

To produce the OsSNDP4 protein, the 1875-bp CDS of the *OsSNDP4* gene, including the stop codon, was amplified from the wild-type HHZ anther cDNA using the MBP-OsSNDP4-F and MBP-OsSNDP4-R primer pair. The PCR product was then cloned into the pMAL-c5X-MBP vector to create the MBP-OsSNDP4 protein expression vector. Following sequence confirmation, the plasmid was transformed into the *E. coli* strain *Rosetta* (DE3). The expression of the MBP-OsSNDP4 fusion protein was induced with IPTG and purified using Amylose Resin (NEB, USA). Using the 1875-bp CDS of *OsSNDP4* as a template, PCR amplification was performed to generate DNA fragments coding for the N-terminal partial protein containing the Sec14 domain and the C-terminal partial protein containing the nodulin domain, using the MBP-Sec14-F and MBP-Sec14-R primer pair, as well as the MBP-Nodulin-F and MBP-Nodulin-R primer pair, respectively (Additional file 17: Table S9). These PCR fragments were cloned into the pMAL-c5X-MBP vector to construct plasmids expressing the MBP-Sec14 domain and MBP-nodulin domain proteins. Induction and purification of these proteins were carried out as described for the MBP-OsSNDP4 fusion protein. The MBP protein was also expressed using the pMAL-c5X-MBP empty vector and purified as a control. Protocols for protein expression and purification refer to the pMAL™ Protein Fusion and Purification System Instruction Manual (NEB, USA). The purified proteins were quantified using the Bradford Protein Assay Kit (Beyotime, China) according to the manufacturer's instructions.

Procedures described by Deng et al. (2016) were referenced for the protein-lipid blot overlay assay. Briefly, 25 μg MBP fusion proteins were diluted in 8 mL blocking buffer and incubated with membrane lipid strips (Echelon Biosciences, USA) for 2 h. After incubation, the membrane was probed with a 1:8000 dilution of Anti-MBP monoclonal antibody (TransGen Biotech, China), followed by washing to remove unbound antibody. The membrane was then incubated with a 1:5000 dilution of anti-mouse antibody (TransGen Biotech, China) and washed again. The Easysee® Western Blot Kit (TransGen Biotech, China) and the Tanon 5200 chemiluminescent imaging system (Tanon, China) were used to visualize the hybridization signal on the membrane.

RNA-seq and Comparative Transcriptome Analysis

Total RNA was extracted from stage 9 anthers from the WT HHZ and *ms16600* mutant using TRIzol reagent (Invitrogen). RNA-seq libraries were constructed and sequenced on the Illumina Hi-Seq 2000 platform according to the manufacturer's instructions, resulting in the generation of >7 Gb of data. The raw data were cleaned by trimming off sequencing adaptors and removing poor-quality sequences to yield clean reads. These clean reads were aligned to the IRGSP 1.0 rice genome using STAR v2.5.2b (Dobin et al. 2013). Gene counting was performed Using featureCounts v2.0.1 (Liao et al. 2014). The DEGs were identified using the DESeq2 R package with a P-value≤0.05 and an absolute $\log_2$ fold change greater than 1 (Wang et al. 2010). The DEGs were annotated using KofamKOALA for KEGG pathway mapping (Aramaki et al. 2020). Subsequent enrichment analysis was performed on the annotated genes to identify significant biological pathways and processes.

Abbreviations

ABCG	ATP binding cassette G
ACOS	Acyl-coa synthase
AtSFH	Arabidopsis thaliana Sec14 homolog
CER1/3/6	Eceriferum1/3/6
CUT1	Cutinase1
CYP703A3	Cytochrome P450 703A3
CYP704B2	Cytochrome P450 704B2
DPW	Defective pollen wall
DPW2	Defective pollen wall 2
ED	Euclidean distance
EMS	Ethyl methanesulfonate
ER	Endoplasmic reticulum
HHZ	Huanghuazhan
HRM	High resolution melting
KEGG	Kyoto encyclopedia of genes and genomes
LACS	Long-chain acyl-CoA synthetase
LAP5/6	Less adhesive pollen
LPA	Lysophosphatidic acid
LPC	Lysophosphocholine
LTP	Lipid transfer protein
MMC	Microspore mother cell
GPAT3	Glycerol-3-phosphate acyltransferase 3
OsNP1	Oryza sativa No Pollen 1
OsPKS1/2	Oryza sativa polyketide synthase ½
OsSNDP	Oryza sativa Sec14-nodulin domain protein
PA	Phosphatidic acid
PC	Phosphatidylcholine
PE	Phosphatidylethanolamine
PG	Phosphatidylglycerol
PI(3)P	Phosphatidylinositol(3)-phosphate
$PI(3,4)P_2$	Phosphatidylinositol(3,4)-bisphosphate
$PI(3,4,5)P_3$	Phosphatidylinositol(3,4,5)-trisphosphate
$PI(3,5)P_2$	Phosphatidylinositol(3,5)-bisphosphate
PI(4)P	Phosphatidylinositol(4)-phosphate
$PI(4,5)P_2$	Phosphatidylinositol(4,5)-bisphosphate
PI(5)P	Phosphatidylinositol (5)-phosphate
PI	Phosphatidylinositol
PI3K	Phosphatidylinositol 3-kinase
PKSA/B	Polyketide synthase A/B
PS	Phosphatidylserine
qRT	PCR-Quantitative reverse transcription-PCR
S1P	Sphingosine 1-Phosphate
Sec14L	PITPs-Sec14-like PI transfer proteins
SIMM	Simultaneous Identification of Multiple Causal Mutations
SM	Sphingomyelin
SNP	Single nucleotide polymorphism
TDR	Tapetum degeneration retardation
TKPR1/2	Tetraketide reductase ½
WDA1	Wax-deficient anther 1

Supplementary Information

The online version contains supplementary material available at https://doi.org/10.1186/s12284-024-00730-y.

Supplementary Material 1

Supplementary Material 2

Acknowledgements

We thank the Microscope Center in Life Science School of Sun Yat-sen University for using their facilities for microscopic analysis, Yao-Guang Liu in South China Agriculture University for the CRISPR/Cas9 system, and Xin Peng in Guangdong Academy of Agricultural Sciences for assistance in RNA-seq data analysis.

Author Contributions

WX, XP, XZ, and SC conducted mutant isolation, phenotypic analysis, gene complementation, CRISPR knockout, gene expression, protein lipid overlay assay, and protein sequence analysis. CW and WX conducted protein subcellular localization; WY and CRW conducted SIMM assay and RNA-seq assay; YL conducted microscopy and figure design; CX and XT designed the experiments, analyzed the data, and wrote the manuscript. SC reviewed and edited the paper. XT and SC obtained funds. All authors read and approved the manuscript for publication.

Funding

This work was supported by Guangdong Laboratory of Lingnan Modern Agriculture Project (NZ2021003), National Natural Science Foundation of China (32370362), Guangdong Basic and Applied Basic Research Foundation (2023B1515120050 and 2022A1515110457), and the Major Program of Guangdong Basic and Applied Research (2019B030302006).

Data Availability

No datasets were generated or analysed during the current study.

Declarations

Ethics approval and consent to participate

Not applicable.

Consent for publication

Not applicable.

Competing Interests

The authors declare no competing interests.

Received: 14 June 2024 / Accepted: 6 August 2024
Published online: 29 August 2024

References

Aarts MG, Keijzer CJ, Stiekema WJ, Pereira A (1995) Molecular characterization of the CER1 gene of Arabidopsis involved in epicuticular wax biosynthesis and pollen fertility. Plant Cell 7:2115–2127

Aramaki T, Blanc-Mathieu R, Endo H, Ohkubo K, Kanehisa M, Goto S, Ogata H (2020) KofamKOALA: KEGG ortholog assignment based on profile HMM and adaptive score threshold. Bioinformatics 36:2251–2252

Ariizumi T, Toriyama K (2011) Genetic regulation of sporopollenin synthesis and pollen exine development. Annu Rev Plant Biol 62:437–460

Bankaitis VA, Malehorn DE, Emr SD, Greene R (1989) The Saccharomyces cerevisiae Sec14 gene encodes a cytosolic factor that is required for transport of secretory proteins from the yeast golgi complex. J Cell Biol 108:1271–1281

Bankaitis VA, Aitken JR, Cleves AE, Dowhan W (1990) An essential role for a phospholipid transfer protein in yeast golgi function. Nature 347:561–562
Bankaitis VA, Mousley CJ, Schaaf G (2010) The Sec14 superfamily and mechanisms for crosstalk between lipid metabolism and lipid signaling. Trends Biochem Sci 35:150–160
Böhme K, Li Y, Charlot F, Grierson C, Marrocco K, Okada K, Laloue M, Nogué F (2004) The Arabidopsis COW1 gene encodes a phosphatidylinositol transfer protein essential for root hair tip growth. Plant J 40:686–698
Brown WJ, DeWald DB, Emr SD, Plutner H, Balch WE (1995) Role for phosphatidylinositol 3-kinase in the sorting and transport of newly synthesized lysosomal enzymes in mammalian cells. J Cell Biol 130:781–796
Bunney TD, Watkins PA, Beven AF, Shaw PJ, Hernandez LE, Lomonossoff GP, ShanksM, Peart J, Drøbak BK (2000) Association of phosphatidylinositol 3-kinase with nuclear transcription sites in higher plants. Plant Cell 12:1679–1688
Chang Z, Chen Z, Wang N, Xie G, Lu J, Yan W, Zhou J, Tang X, Deng XW (2016a) Construction of a male sterility system for hybrid rice breeding and seed production using a nuclear male sterility gene. Proc Natl Acad Sci U S A 113:14145–14150
Chang Z, Chen Z, Yan W, Xie G, Lu J, Wang N, Lu Q, Yao N, Yang G, Xia J, Tang X (2016b) An ABC transporter, OsABCG26, is required for anther cuticle and pollen exine formation and pollen-pistil interactions in rice. Plant Sci 253:21–30
Chang Z, Jin M, Yan W, Chen H, Qiu S, Fu S, Xia J, Liu Y, Chen Z, Wu J, Tang X (2018) The ATP-binding cassette (ABC) transporter OsABCG3 is essential for pollen development in rice. Rice (N Y) 11:58
Chen S, Tao L, Zeng L, Vega-Sanchez ME, Umemura K, Wang GL (2006) Mol Plant Pathol. A highly efficient transient protoplast system for analyzing defence gene expression and protein-protein interactions in rice. 7:417–427
Chen Z, Lu J, Lu Q, Wang N, Wang C, Xie G, Zhou X, Tang X (2014) Screening and analysis of male sterile mutants derived from elite indica cultivar Huanghuazhan. Guangdong Agri Sci 41:1–4
Chen X, Zhang H, Sun H, Luo H, Zhao L, Dong Z, Yan S, Zhao C, Liu R, Xu C, Li S, Chen H, Jin W (2017) IRREGULAR POLLEN EXINE1 is a novel factor in anther cuticle and pollen exine formation. Plant Physiol 173:307–325
Chen L, Ji C, Zhou D, Gou X, Tang J, Jiang Y, Han J, Liu YG, Chen L, Xie Y (2022) OsLTP47 may function in a lipid transfer relay essential for pollen wall development in rice. J Genet Genomics 49:481–491
Choi H, Ohyama K, Kim YY, Jin JY, Lee SB, Yamaoka Y, Muranaka T, Suh MC, Fujioka S, Lee Y (2014) The role of Arabidopsis ABCG9 and ABCG31 ATP binding cassette transporters in pollen fitness and the deposition of steryl glycosides on the pollen coat. Plant Cell 26:310–324
Chu M, Li J, Zhang J, Shen S, Li C, Gao Y, Zhang S (2018) AtCaM4 interacts with a Sec14-like protein, PATL1, to regulate freezing tolerance in Arabidopsis in a CBF-independent manner. J Exp Bot 69:5241–5253
daSilva LLP, Taylor JP, Hadlington JL, Hanton SL, Snowden CJ, Fox SJ, Foresti O, Brandizzi F, Denecke J (2005) Receptor salvage from the prevacuolar compartment is essential for efficient vacuolar protein targeting. Plant Cell 17:132–148
Davidson HW (1995) Wortmannin causes mistargeting of procathepsin D: evidence for the involvement of a phosphatidylinositol 3-kinase in vesicular transport to lysosomes. J Cell Biol 130:797–805
de Azevedo Souza C, Kim SS, Koch S, Kienow L, Schneider K, McKim SM, Haughn GW, Kombrink E, Douglas CJ (2009) A novel fatty Acyl-CoA synthetase is required for pollen development and sporopollenin biosynthesis in Arabidopsis. Plant Cell 21:507–525
Deng T, Yao H, Wang J, Wang J, Xue H, Zuo K (2016) GhLTPG1, a cotton GPI-anchored lipid transfer protein, regulates the transport of phosphatidylinositol monophosphates and cotton fiber elongation. Sci Rep 6:26829
Dobin A, Davis CA, Schlesinger F, Drenkow J, Zaleski C, Jha S, Batut P, Chaisson M, Gingeras TR (2013) STAR: ultrafast universal RNA-seq aligner. Bioinformatics 29:15–21
Dobritsa AA, Shrestha J, Morant M, Pinot F, Matsuno M, Swanson R, Moller BL, Preuss D (2009) CYP704B1 is a long-chain fatty acid omega-hydroxylase essential for sporopollenin synthesis in pollen of Arabidopsis. Plant Physiol 151:574–589
Dobritsa AA, Lei Z, Nishikawa S, Urbanczyk-Wochniak E, Huhman DV, Preuss D, Sumner LW (2010) LAP5 and LAP6 encode anther-specific proteins with similarity to chalcone synthase essential for pollen exine development in Arabidopsis. Plant Physiol 153:937–955
Edstam MM, Edqvist J (2014) Involvement of GPI-anchored lipid transfer proteins in the development of seed coats and pollen in Arabidopsis thaliana. Physiol Plant 152:32–42
Fang C, Wu S, Li Z, Pan S, Wu Y, An X, Long Y, Wei X, Wan X (2023) A systematic investigation of lipid transfer proteins involved in male fertility and other biological processes in maize. Int J Mol Sci 24:1660
Fiebig A, Mayfield JA, Miley NL, Chau S, Fischer RL, Preuss D (2000) Alterations in CER6, a gene identical to CUT1, differentially affect long-chain lipid content on the surface of pollen and stems. Plant Cell 12:2001–2008
Gerth K, Lin F, Menzel W, Krishnamoorthy P, Stenzel I, Heilmann M, Heilmann I (2017) Guilt by association: a phenotype-based view of the plant phosphoinositide network. Annu Rev Plant Biol 68:349–374
Ghosh R, de Campos MK, Huang J, Huh SK, Orlowski A, Yang Y, Tripathi A, Nile A, Lee HC, Dynowski M, Schäfer H, Róg T, Lete MG, Ahyayauch H, Alonso A, Vattulainen I, Igumenova TI, Schaaf G, Bankaitis VA (2015) Sec14-nodulin proteins and the patterning of phosphoinositide landmarks for developmental control of membrane morphogenesis. Mol Biol Cell 26:1764–1781
Grienenberger E, Quilichini TD (2021) The toughest material in the plant kingdom: an update on sporopollenin. Front Plant Sci 12:703864
Grienenberger E, Kim SS, Lallemand B, Geoffroy P, Heintz D, Souza Cde A, Heitz T, Douglas CJ, Legrand M (2010) Analysis of TETRAKETIDE alpha-PYRONE REDUCTASE function in Arabidopsis thaliana reveals a previously unknown, but conserved, biochemical pathway in sporopollenin monomer biosynthesis. Plant Cell 22:4067–4083
Grierson CS, Roberts K, Feldmann KA, Dolan L (1997) The COW1 locus of Arabidopsis acts after RHD2, and in parallel with RHD3 and TIP1, to determine the shape, rate of elongation, and number of root hairs produced from each site of hair formation. Plant Physiol 115:981–990
Hammond GR, Balla T (2015) Polyphosphoinositide binding domains: key to inositol lipid biology. Biochim et Biophys Acta 1851:746–758
Heilmann I (2016) Phosphoinositide signaling in plant development. Development 143:2044–2055
Hertle AP, García-Cerdán JG, Armbruster U, Shih R, Lee JJ, Wong W, Niyogi KK (2020) A Sec14 domain protein is required for photoautotrophic growth and chloroplast vesicle formation in Arabidopsis thaliana. Proc Natl Acad Sci USA 117:9101–9111
Holič R, Šťastný D, Griač P (2021) Sec14 family of lipid transfer proteins in yeasts. Biochim Biophys Acta Mol Cell Biol Lipids 1866:158990
Hsieh K, Huang AH (2005) Lipid-rich tapetosomes in Brassica Tapetum are composed of oleosin-coated oil droplets and vesicles, both assembled in and then detached from the endoplasmic reticulum. Plant J 43:889–899
Hsieh K, Huang AH (2007) Tapetosomes in Brassica Tapetum accumulate endoplasmic reticulum-derived flavonoids and alkanes for delivery to the pollen surface. Plant Cell 19:582–596
Huang MD, Chen TL, Huang AH (2013a) Abundant type III lipid transfer proteins in Arabidopsis tapetum are secreted to the locule and become a constituent of the pollen exine. Plant Physiol 163:1218–1229
Huang J, Kim CM, Xuan Y-H, Park SJ, Piao HL, Je BI, Liu J, Kim TH, Kim B-K, Han C-D (2013b) OsSNDP1, a Sec14-nodulin domain-containing protein, plays a critical role in root hair elongation in rice. Plant Mol Biol 82:39–50
Huang J, Ghosh R, Bankaitis VA (2016a) Sec14-like phosphatidylinositol transfer proteins and the biological landscape of phosphoinositide signaling in plants. Acta Biochim Biophys Sin 1861:1352–1364
Huang J, Ghosh R, Tripathi A, Lonnfors M, Somerharju P, Bankaitis VA (2016b) Two-ligand priming mechanism for potentiated phosphoinositide synthesis is an evolutionarily conserved feature of Sec14-like phosphatidylinositol and phosphatidylcholine exchange proteins. Mol Biol Cell 27:2317–2330
Huysmans S, El-Ghazaly G, Smets E (1998) Orbicules in Angiosperms: morphology, function, distribution, and relation with tapetum types. Bot Rev 64:240–272
Irvine RF (2016) A short history of inositol lipids. J Lipid Res 57:1987–1994
Jessen D, Olbrich A, Knufer J, Kruger A, Hoppert M, Polle A, Fulda M (2011) Combined activity of LACS1 and LACS4 is required for proper pollen coat formation in Arabidopsis. Plant J 68:715–726
Jiao L, Liu Y, Yu XY, Pan X, Zhang Y, Tu J, Song YH, Li Y (2023) Ribosome biogenesis in disease: new players and therapeutic targets. Sig Transduct Target Ther 8:15
Jung KH, Han MJ, Lee DY, Lee YS, Schreiber L, Franke R, Faust A, Yephremov A, Saedler H, Kim YW, Hwang I, An G (2006) Wax-deficient anther1 is involved in cuticle and wax production in rice anther walls and is required for pollen development. Plant Cell 18:3015–3032
Kim DH, Eu YJ, Yoo CM, Kim YW, Pih KT, Jin JB, Kim SJ, Stenmark H, Hwang I (2001) Trafficking of phosphatidylinositol 3-phosphate from the trans-golgi network to the lumen of the central vacuole in plant cells. Plant Cell 13:287–301
Kim SS, Grienenberger E, Lallemand B, Colpitts CC, Kim SY, Souza Cde A, Geoffroy P, Heintz D, Krahn D, Kaiser M, Kombrink E, Heitz T, Suh DY, Legrand M, Douglas

CJ (2010) LAP6/POLYKETIDE SYNTHASE A and LAP5/POLYKETIDE SYNTHASE B encode hydroxyalkyl alpha-pyrone synthases required for pollen development and sporopollenin biosynthesis in Arabidopsis thaliana. Plant Cell 22:4045–4066

Kim EH, Poudyal RS, Lee KR, Yu H, Gi E, Kim HU (2022) Chloroplast-localized PITP7 is essential for plant growth and photosynthetic function in Arabidopsis. Physiol Plant 174:e13760

Kumar S, Stecher G, Li M, Knyaz C, Tamura K (2018) MEGA X: Molecular Evolutionary Genetics Analysis across Computing platforms. Mol Biol Evol 35:1547–1549

Lebecq A, Doumane M, Fangain A, Bayle V, Leong JX, Rozier F, Marques-Bueno MD, Armengot L, Boisseau R, Simon ML, Franz-Wachtel M, Macek B, Üstün S, Jaillais Y, Caillaud MC (2022) The Arabidopsis SAC9 enzyme is enriched in a cortical population of early endosomes and restricts PI(4,5)P2 at the plasma membrane. Elife 11:e73837

Lee Y, Kim ES, Choi Y, Hwang I, Staiger CJ, Chung YY, Lee Y (2008) The Arabidopsis phosphatidylinositol 3-kinase is important for pollen development. Plant Physiol 147:1886–1897

Li N, Zhang DS, Liu HS, Yin CS, Li XX, Liang WQ, Yuan Z, Xu B, Chu HW, Wang J, Wen TQ, Huang H, Luo D, Ma H, Zhang DB (2006) The rice tapetum degeneration retardation gene is required for tapetum degradation and anther development. Plant Cell 18:2999–3014

Li H, Pinot F, Sauveplane V, Werck-Reichhart D, Diehl P, Schreiber L, Franke R, Zhang P, Chen L, Gao Y, Liang W, Zhang D (2010a) Cytochrome P450 family member CYP704B2 catalyzes the ω-hydroxylation of fatty acids and is required for anther cutin biosynthesis and pollen exine formation in rice. Plant Cell 22:173–190

Li H, Yuan Z, Vizcay-Barrena G, Yang C, Liang W, Zong J, Wilson ZA, Zhang D (2011) PERSISTENT TAPETAL CELL1 encodes a PHD-finger protein that is required for tapetal cell death and pollen development in rice. Plant Physiol 156:615–630

Li XC, Zhu J, Yang J, Zhang GR, Xing WF, Zhang S, Yang ZN (2012) Glycerol-3-phosphate acyltransferase 6 (GPAT6) is important for tapetum development in Arabidopsis and plays multiple roles in plant fertility. Mol Plant 5:131–142

Li Y, Li D, Guo Z, Shi Q, Xiong S, Zhang C, Zhu J, Yang Z (2016) OsACOS12, an orthologue of Arabidopsis acyl-CoA synthetase5, plays an important role in pollen exine formation and anther development in rice. BMC Plant Biol 16:256

Li FS, Phyo P, Jacobowitz J, Hong M, Weng JK (2019) The molecular structure of plant sporopollenin. Nat Plants 5:41–46

Li H, Kim YJ, Yang L, Liu Z, Zhang J, Shi H, Huang G, Persson S, Zhang D, Liang W (2020) Grass-specific *EPAD1* is essential for pollen exine patterning in rice. Plant Cell 32:3961–3977

Li J, Wang Z, Chang Z, He H, Tang X, Ma L, Deng XW (2021) A functional characterization of TaMs1 orthologs in Poaceae plants. Crop J 9:1291–1300

Liao Y, Smyth GK, Shi W (2014) FeatureCounts: an efficient general purpose program for assigning sequence reads to genomic features. Bioinformatics 30:923–930

Liu L, Fan XD (2013) Tapetum: regulation and role in sporopollenin biosynthesis in Arabidopsis. Plant Mol Biol 83:165–175

Lochlainn SO, Amoah S, Graham NS, Alamer K, Rios JJ, Kurup S, Stoute A, Hammond JP, Ostergaard L, King GJ, White PJ, Broadley MR (2011) High Resolution Melt (HRM) analysis is an efficient tool to genotype EMS mutants in complex crop genomes. Plant Methods 7:43

Ma X, Zhang Q, Zhu Q, Liu W, Chen Y, Qiu R, Wang B, Yang Z, Li H, Lin Y, Xie Y, Shen R, Chen S, Wang Z, Chen Y, Guo J, Chen L, Zhao X, Dong Z, Liu YG (2015) A robust CRISPR/Cas9 system for convenient, high-efficiency multiplex genome editing in monocot and dicot plants. Mol Plant 8:1274–1284

Matsuoka K, Bassham DC, Raikhel NV, Nakamura K (1995) Different sensitivity to wortmannin of two vacuolar sorting signals indicates the presence of distinct sorting machineries in tobacco cells. J Cell Biol 130:1307–1318

Men X, Shi J, Liang W, Zhang Q, Lian G, Quan S, Zhu L, Luo Z, Chen M, Zhang D (2017) Glycerol-3-Phosphate acyltransferase 3 (OsGPAT3) is required for anther development and male fertility in rice. J Exp Bot 68:513–526

Montag K, Hornbergs J, Ivanov R, Bauer P (2020) Phylogenetic analysis of plant multi-domain Sec14-like phosphatidylinositol transfer proteins and structure–function properties of PATELLIN2. Plant Mol Biol 104:665–678

Montag K, Ivanov R, Bauer P (2023) Role of Sec14-like phosphatidylinositol transfer proteins in membrane identity and dynamics. Front Plant Sci 14:1181031

Moon S, Kim YJ, Park HE, Kim J, Gho YS, Hong WJ, Kim EJ, Lee SK, Suh BC, An G, Jung KH (2022) OsSNDP3 functions for the Polar Tip Growth in Rice Pollen together with OsSNDP2, a paralog of OsSNDP3. Rice (N Y) 15:39

Morant M, Jorgensen K, Schaller H, Pinot F, Moller BL, Werck-Reichhart D, Bak S (2007) CYP703 is an ancient cytochrome P450 in land plants catalyzing in-chain hydroxylation of lauric acid to provide building blocks for sporopollenin synthesis in pollen. Plant Cell 19:1473–1487

Mousley CJ, Davison JM, Bankaitis VA (2012) Sec14 like PITPs couple lipid metabolism with phosphoinositide synthesis to regulate Golgi functionality. Subcell Biochem 59:271–287

Ni E, Zhou L, Li J, Jiang D, Wang Z, Zheng S, Qi H, Zhou Y, Wang C, Xiao S et al (2018) OsCER1 plays a pivotal role in very long-chain alkane biosynthesis and affects plastid development and programmed cell death of tapetum in rice (*Oryza sativa* L). Front Plant Sci 9:1217

Niu BX, He FR, He M, Ren D, Chen LT, Liu YG (2013a) The ATP-binding cassette transporter OsABCG15 is required for anther development and pollen fertility in rice. J Integr Plant Biol 55:710–720

Niu N, Liang W, Yang X, Jin W, Wilson ZA, Hu J, Zhang D (2013b) EAT1 promotes tapetal cell death by regulating aspartic proteases during male reproductive development in rice. Nat Commun 4:1445

Noack LC, Jaillais Y (2020) Functions of anionic lipids in plants. Annu Rev Plant Biol 71:71–102

Panikashvili D, Shi JX, Bocobza S, Franke RB, Schreiber L, Aharoni A (2010) The Arabidopsis DSO/ABCG11 transporter affects cutin metabolism in reproductive organs and suberin in roots. Mol Plant 3:563–575

Peterman TK, Ohol YM, McReynolds LJ, Luna EJ (2004) Patellin1, a novel Sec14-like protein, localizes to the cell plate and binds phosphoinositides. Plant Physiol 136:3080–3094

Qiao Y, Hou B, Qi X (2023) Biosynthesis and transport of pollen coat precursors in angiosperms. Nat Plants 9:864–876

Qin P, Tu B, Wang Y, Deng L, Quilichini TD, Li T, Wang H, Ma B, Li S (2013) ABCG15 encodes an ABC transporter protein, and is essential for post-meiotic anther and pollen exine development in rice. Plant Cell Physiol 54:138–154

Quilichini TD, Friedmann MC, Samuels AL, Douglas CJ (2010) ATP-binding cassette transporter G26 is required for male fertility and pollen exine formation in Arabidopsis. Plant Physiol 154:678–690

Quilichini TD, Samuels AL, Douglas CJ (2014) ABCG26-mediated polyketide trafficking and hydroxycinnamoyl spermidines contribute to pollen wall exine formation in Arabidopsis. Plant Cell 26:4483–4498

Reszczyńska E, Hanaka A (2020) Lipids composition in plant membranes. Cell Biochem Biophys 78:401–414

Román-Fernández Á, Roignot J, Sandilands E, Nacke M, Mansour MA, McGarry L, Shanks E, Mostov KE, Bryant DM (2018) The phospholipid PI(3,4)P2 is an apical identity determinant. Nat Commun 9:5041

Rowland O, Lee R, Franke R, Schreiber L, Kunst L (2007) The CER3 wax biosynthetic gene from Arabidopsis thaliana is allelic to WAX2/YRE/FLP1. FEBS Lett 581:3538–3544

Schaaf G, Ortlund EA, Tyeryar KR, Mousley CJ, Ile KE, Garrett TA, Ren J, Woolls MJ, Raetz CR, Redinbo MR, Bankaitis VA (2008) Functional anatomy of phospholipid binding and regulation of phosphoinositide homeostasis by proteins of the Sec14 superfamily. Mol Cell 29:191–206

Shi J, Cui M, Yang L, Kim YJ, Zhang D (2015) Genetic and biochemical mechanisms of pollen wall development. Trends Plant Sci 20:741–753

Simon ML, Platre MP, Assil S, van Wijk R, Chen WY, Chory J, Dreux M, Munnik T, Jaillais Y (2014) A multi-colour/multi-affinity marker set to visualize phosphoinositide dynamics in Arabidopsis. Plant J 77:322–337

Stack JH, Emr SD (1994) Vps34p required for yeast vacuolar protein sorting is a multiple specificity kinase that exhibits both protein kinase and PtdIns-specific PI 3-kinase activities. J Biol Chem 269:31552–31562

Sun L, Xiang X, Yang Z, Yu P, Wen X, Wang H, Abbas A, Muhammad Khan R, Zhang Y, Cheng S, Cao L (2018) OsGPAT3 plays a critical role in anther wall programmed cell death and pollen development in rice. Int J Mol Sci 19:4017

Tejos R, Rodriguez-Furlan C, Adamowski M, Sauer M, Norambuena L, Friml J (2017) PATELLINS are regulators of auxin-mediated PIN1 relocation and plant development in Arabidopsis thaliana. J Cell Sci 131:jcs204198

Tse YC, Mo B, Hillmer S, Zhao M, Lo SW, Robinson DG, Jiang L (2004) Identification of multivesicular bodies as prevacuolar compartments in Nicotiana tabacum BY-2 cells. Plant Cell 16:672–693

van Leeuwen W, Vermeer JE, Gadella TW Jr, Munnik T (2007) Visualization of phosphatidylinositol 4,5-bisphosphate in the plasma membrane of suspension-cultured tobacco BY-2 cells and whole Arabidopsis seedlings. Plant J 52:1014–1026

Vermeer JE, van Leeuwen W, Tobeña-Santamaria R, Laxalt AM, Jones DR, Divecha N, Gadella TW Jr, Munnik T (2006) Visualization of PtdIns3P dynamics in living plant cells. Plant J 47:687–700

Vermeer JE, Thole JM, Goedhart J, Nielsen E, Munnik T, Gadella TW Jr. (2009) Imaging phosphatidylinositol 4-phosphate dynamics in living plant cells. Plant J 57:356–372
Vincent P, Chua M, Nogue F, Fairbrother A, Mekeel H, Xu Y, Allen N, Bibikova TN, Gilroy S, Bankaitis VA (2005) A Sec14p-nodulin domain phosphatidylinositol transfer protein polarizes membrane growth of Arabidopsis thaliana root hairs. J Cell Biol 168:801–812
Virgili-López G, Langhans M, Bubeck J, Pedrazzini E, Gouzerh G, Neuhaus J-M, Robinson D, Vitale A (2013) Comparison of membrane targeting strategies for the Accumulation of the human immunodeficiency virus p24 protein in transgenic Tobacco. Int J Mol Sci 14:13241–13265
Wan X, Wu S, Li Z, An X, Tian Y (2020) Lipid metabolism: critical roles in male fertility and other aspects of reproductive development in plants. Mol Plant 13:955–983
Wang L, Feng Z, Wang X, Wang X, Zhang X (2010) DEGseq: an R package for identifying differentially expressed genes from RNA-seq data. Bioinformatics 26:136–138
Welters P, Takegawa K, Emr SD, Chrispeels MJ (1994) ATVPS34, a PtdIns 3-kinase of Arabidopsis thaliana is an essential protein with homology to a calcium-dependent lipid-binding domain. Proc Natl Acad Sci USA 91:11398–11402
Whitley P, Hinz S, Doughty J (2009) Arabidopsis FAB1/PIKfyve proteins are essential for development of viable pollen. Plant Physiol 151:1812–1822
Wu L, Guan Y, Wu Z, Yang K, Lv J, Converse R, Huang Y, Mao J, Zhao Y, Wang Z, Min H, Kan D, Zhang Y (2014) OsABCG15 encodes a membrane protein that plays an important role in anther cuticle and pollen exine formation in rice. Plant Cell Rep 33:1881–1899
Xu D, Shi J, Rautengarten C, Yang L, Qian X, Uzair M, Zhu L, Luo Q, An G, Wassmann F, Schreiber L, Heazlewood JL, Scheller HV, Hu J, Zhang D, Liang W (2017) Defective Pollen Wall 2 (DPW2) encodes an acyl transferase required for rice pollen development. Plant Physiol 173:240–255
Xu D, Qu S, Tucker MR, Zhang D, Liang W, Shi J (2019) *Ostkpr1* functions in anther cuticle development and pollen wall formation in rice. BMC Plant Biol 19:104
Yadav V, Molina I, Ranathunge K, Castillo IQ, Rothstein SJ, Reed JW (2014) ABCG transporters are required for suberin and pollen wall extracellular barriers in Arabidopsis. Plant Cell 26:3569–3588
Yan W, Chen Z, Lu J, Xu C, Xie G, Li Y, Deng XW, He H, Tang X (2017) Simultaneous identification of multiple causal mutations in Rice. Front Plant Sci 7:2055
Yang X, Wu D, Shi J, He Y, Pinot F, Grausem B, Yin C, Zhu L, Chen M, Luo Z, Liang W, Zhang D (2014) Rice CYP703A3, a cytochrome P450 hydroxylase, is essential for development of anther cuticle and pollen exine. J Integr Plant Biol 56:979–994
Yang X, Liang W, Chen M, Zhang D, Zhao X, Shi J (2017) Rice fatty acyl-CoA synthetase OsACOS12 is required for tapetum programmed cell death and male fertility. Planta 246:105–122
Yang M, Sakruaba Y, Ishikawa T, Ohtsuki N, Kawai-Yamada M, Yanagisawa S (2023) Chloroplastic Sec14-like proteins modulate growth and phosphate deficiency responses in Arabidopsis and rice. Plant Physiol 192:3030–3048
Yao HY, Lu YQ, Yang XL, Wang XQ, Luo Z, Lin DL, Wu JW, Xue HW (2023) Arabidopsis Sec14 proteins (SFH5 and SFH7) mediate interorganelle transport of phosphatidic acid and regulate chloroplast development. Proc Natl Acad Sci USA 120:e2221637120
Zhai C, Zhang Y, Yao N, Lin F, Liu Z, Dong Z, Wang L, Pan Q (2014) Function and interaction of the coupled genes responsible for Pik-h encoded rice blast resistance. PLoS ONE 9:e98067
Zhang D, Liang W, Yin C, Zong J, Gu F, Zhang D (2010) OsC6, encoding a lipid transfer protein, is required for postmeiotic anther development in rice. Plant Physiol 154:149–162
Zhang D, Luo X, Zhu L (2011) Cytological analysis and genetic control of rice anther development. J Genet Genomics 38:379–390
Zhao G, Shi J, Liang W, Xue F, Luo Q, Zhu L, Qu G, Chen M, Schreiber L, Zhang D (2015) Two ATP binding Cassette G transporters, rice ATP Binding Cassette G26 and ATP binding Cassette G15, collaboratively regulate rice male reproduction. Plant Physiol 169:2064–2079
Zheng Z, Xia Q, Dauk M, Shen W, Selvaraj G, Zou J (2003) Arabidopsis AtGPAT1, a member of the membrane-bound glycerol-3- phosphate acyltransferase gene family, is essential for tapetum differentiation and male fertility. Plant Cell 15:1872–1887
Zhou H, Wang C, Tan T, Cai J, He J, Lin H (2018) Patellin1 negatively modulates salt tolerance by regulating PM Na+/H + antiport activity and cellular redox homeostasis in Arabidopsis. Plant Cell Physiol 59:1630–1642
Zhu X, Yu J, Shi J, Tohge T, Fernie AR, Meir S, Aharoni A, Xu D, Zhang D, Liang W (2017) The polyketide synthase OsPKS2 is essential for pollen exine and Ubisch body patterning in rice. J Integr Plant Biol 59:612–628

Publisher's Note